2016

The effect of glycerol on readily biodegradable chemical oxygen demand (RBCOD) in a wastewater stream

Rojina Rawut
University of Central Florida

THE EFFECT OF GLYCEROL ON READILY BIODEGRADABLE CHEMICAL OXYGEN DEMAND (RBCOD) IN A WASTEWATER STREAM

by

ROJINA RAWUT
M.Sc. School of Environmental Science and Management (SchEMS), 2009

A thesis submitted in partial fulfillment of the requirements
for the degree of Master of Science
in the Department of Civil, Environmental and Construction Engineering
in the College of Engineering and Computer Science
at the University of Central Florida
Orlando, Florida

Spring Term
2016

Major Professor: Anwar Sadmani

ABSTRACT

This study evaluated the short-term effects of glycerol addition on readily biodegradable (RB) chemical oxygen demand (COD) in a carbon limited wastewater influent. The presence of an RB fraction provides with a suitable substrate for microorganisms to produce volatile fatty acids (VFA). The oxygen utilization rate (OUR) has been used to evaluate the oxygen consumption for RB substrate in wastewater. Wastewater with low organic content contains limited RB substrate, and thus, additional carbon source is required to improve biological treatment capability. Acetate, propionate, methanol, and glycerol are the commonly available carbon sources for biological treatment process. However, the cost of acetate and propionate are relatively high, and it is not economical to use these carbon sources in the wastewater plant. The use of methanol as a carbon source inherently poses safety issues in field applications due to its toxic and flammable properties. On the other hand, crude glycerol is the byproduct of biodiesel, which is an excellent carbon source alternative. However, crude glycerol contains impurities and requires a certain degree of purification to enhance the performance.

The samples for the study were collected from the Iron Bridge Wastewater Reclamation Facility (Oviedo, FL) designed for treating municipal wastewater. The total COD (TCOD) of the sample influent was in the range of 237 to 408 mg COD/L, and RBCOD value was between 38 and 80.5 mg COD/L, containing up to 10 mg COD/L of VFA. This study also demonstrates the relationship between the glycerol concentration and OURs during the diauxic growth phase from the addition of glycerol. The growth was due to the existence of RB substrate and availability of glycerol for the microorganisms. TCOD increased from 284 to 378 mg COD/L and from 284 mg

COD/L to 323 mg COD/L by spiking approximately 30 and 15 mL of glycerol stock solution (6.67 g/L), respectively. RBCOD increased from 45 to 89 mg COD/L and 55 mg COD/ L by spiking 30 mL and 15 ml glycerol stock solution, respectively. The initial influent heterotrophic active biomass (Z_{BH}) increased from 5.4 to 15.8 mg VSS/L (8 to 23.4 mg COD/L) due to the addition of glycerol, indicating that the glycerol may be an adequate carbon source. The COD of wastewater with limited VFA (e.g., 10 mg COD/L) increased up to 2,502 mg COD/L where propionic acid (2,468 mg COD/L) exists as the primary end product with a small quantity of acetic acid (34 mg COD/L). Propionic acid was the main VFA component fermented from the glycerol addition. Glycerol addition led to increased RBCOD accompanied by high VFA production. This research investigated the short-term effect of glycerol addition on existing RBCOD in wastewater. It is recommended to explore the effect of increased RBCOD by the addition of glycerol to the effluent N and P for future study.

Keywords: Wastewater, readily biodegradable oxygen demand (RBCOD), oxygen utilization rate (OUR), Glycerol, biological nutrient removal

ACKNOWLEDGMENTS

It is my great privilege to acknowledge and express the deep gratitude to my advisor Dr. Anwar Sadmani for his effectual guidance. I owe a profound intellectual debt to Dr. Andrew Randall for his ideas and contributions to shaping my thinking on this subject.

I would like to express my gratefulness to my mentor Dr. Jae-Hoon Hwang for providing the stimulus and encouragement in writing this thesis. This thesis would not have completed without his immense effort.

I would also like to thank my committee members Dr. Steven Duranceau and Dr. Woo Hyoung Lee for their review, guidance and support during my studies.

Lastly, I would like to express my sincere thanks to Sultan Salamah, Marzeih Ghasemi and Elizabeth Groves for their laboratory assistance and cooperation to accomplish my course and prepare this thesis.

TABLE OF CONTENTS

LIST OF FIGURES

LIST OF TABLES

LIST OF ABBREVATIONS

AOB = Ammonia Oxidizing Bacteria

BCOD = Biodegradable Chemical Oxygen Demand

BNR = Biological Nutrient Removal

C/N = Carbon/Nitrogen

COD = Chemical Oxygen Demand

COD/N = Chemical Oxygen Demand/Nitrogen

DO = Dissolved Oxygen

DI = Distilled Ionized

DNPAO = Denitrifying Poly Phosphate Accumulating Organism

EBPR= Enhance Biological Phosphorus Removal

ED = Entner-Dudoroff

F-RBCOD = Fermentable Readily Biodegradable Chemical Oxygen Demand

GAOs = Glycogen Accumulating Organisms

G bacteria = Glycogen Bacteria

HAB = Heterotrophic Active Biomass

HRT = Hydraulic Retention Time

3-HV = 3-hydroxyvalerate

LCFA = Long Chain Fatty Acid

LPO = Lactic Producing Organism

MLE = Modified Ludzack Ettinger

MLSS = Mixed Liquor Suspended Solid

NAR = Nitrite Accumulation Ratio

NDAS = Nitrification Denitrification Activated Sludge

NOB = Nitrite Oxidizing Bacteria

NO = Nitric Oxide

N_2O = Nitrous Oxide

OHO = Ordinary Heterotrophic Organism

OUR = Oxygen Utilization Rate

TOC = Total Organic Carbon

TCOD = Total Chemical Oxygen Demand

TP = Total Phosphorus

TSS = Total Suspended Solids

PAO = Polyphosphate Accumulating Organism

PHA = Poly-hydroxy-alkanoate

PHB = Poly-hydroxy-butyrate

PHV = Poly-hydroxy-valerate

RBCOD = Readily Biodegradable Chemical Oxygen Demand

SBCOD = Slowly Biodegradable Chemical Oxygen Demand

SCVFA = Short Chain Volatile Fatty Acid

SRT = Sludge Retention Time

SS = Suspended Solids

TDS = Total Dissolved Solids

TKN = Total Kjeldahl Nitrogen

TN = Total Nitrogen

TP = Total Phosphorus

TS = Total Solids

VFA= Volatile Fatty Acid

VSS = Volatile Suspended Solid

WWTP = Waste Water Treatment Plant

Z_{BH} = Initial Heterotrophic Active Biomass

CHAPTER 1: INTRODUCTION

1.1 Background

In municipal wastewater, the biodegradable substrate that is consumed easily and quickly by the activated sludge is referred to as readily biodegradable chemical oxygen demand (RBCOD). The substrate that is difficult to be degraded by bacteria is considered as slowly biodegradable chemical oxygen demand (SBCOD). RBCOD is further divided into short-chain volatile fatty acids (SCVFAs) and non-SCVFAs, which are represented as volatile fatty acids (VFAs) and fermentable RBCOD (F-RBCOD) (Rossle et al., 2001). RBCOD in raw wastewaters varies from 8 to 25 %, whereas in settled wastewaters from 10 to 35 % of total COD (Henze et al., 2001; Rossle et al., 2001; Orhon et al., 2002; Dauknys et al., 2009). SBCOD constitutes 50 to 70 % of a raw wastewater and 45 to 85 % in the case of a settled wastewater (Rossle et al., 2001). Thus, the characterization of RBCOD provides meaningful information on the biokinetics of an activated sludge system. In an anaerobic zone, RBCOD is easily converted into VFA (Marais et al., 1976). VFA is the primary substrate that is related to synthesis and metabolism for microbial growth. An adequate supply of RBCOD has great importance in the design and operation of N and P removal in denitrification and enhanced biological phosphorus removal (EBPR) (Wentzel et al., 1995). EBPR uses a series of anaerobic and aerobic reactors. In an aerobic condition of EBPR, significant amount of aerobic biomass and suitable substrate (e.g., VFAs) are available (Chu et al., 1994; Randall et al., 1997; Guerrero et al., 2012). For EBPR, SCVFAs are mostly acetic and propionic acids, which are the driving forces of the aerobic microbial metabolism. In denitrification, a more readily biodegradable substrate (RBCOD) is used for the conversion of nitrate to nitrite and drives the higher kinetic rate (Uprety et al., 2013). The recommended range of RBCOD requirement for

the removal of 1 g nitrogen (N) is 4 g to 15 g (Dauknys et al., 2009; Melidis et al., 2009). However, as denitrification processes utilize the available readily biodegradable substrate, the consequent fermentation processes may be hindered (Barnard et al., 2006). Similarly, for phosphorus removal, the suggested minimum ratio is 16:1 for RBCOD/P (Stephens et al., 2004; Dauknys et al., 2009).

In a wastewater, fermentation of the organic compound to VFA by the fermentative organism is the crucial phenomenon for phosphorus and nitrogen removal (Danesh et al., 1997). The municipal waste with low or medium organic content and VFA causes the failure of nutrient removal (Taslie et al., 1999). In order to improve the performance, organic compounds like methanol, ethanol, glycerol, or acetic acid need to be added because of their readily biodegradable characteristics (Cho et al., 2004; Katarzyna et al., 2015). Methanol is the most commonly used external carbon source for denitrification. However, it has safety issues due to its toxic and flammable properties (Lu et al., 2011). Acetic acid is another common carbon source considered but the competition between denitrifying bacteria and polyphosphate accumulating organism (PAO) for carbon affects the nutrient removal (Cho et al., 2004). However, this additional carbon source causes an extra cost and thus it is not economical and hence lower cost alternative sources needs to be considered in wastewater treatment plants (WWTPs).

Crude glycerol is a byproduct of biodiesel, and one kilogram of biodiesel can produce approximately hundred grams of glycerol (Yazdani et al., 2007). The discharge industry derived crude glycerol can significantly affect the hydro-ecosystems. One of the mitigation strategies is to use the crude glycerol as an alternative sustainable carbon source. Crude glycerol contains high

impurities such as salts, VFAs, long-chain fatty acids (LCFAs), and other organic contaminations, resulting in a low commercial value due to its subsequent purification and disposal cost (Yazdani et al., 2007; Taya et al., 2015). Pure glycerol is becoming popular due to its 95 % purity and can be utilized as a source of carbon and energy. Yuan et al. (2010) found that glycerol, when fermented with waste activated sludge, can be used as co-substrate and results in a successful operation of EBPR. Guerrero et al. (2012) stated that in full-scale wastewater treatment plant (WWTP), appropriate anaerobic hydraulic retention time was necessary to use glycerol as a sole carbon source. The study of glycerol in the denitrification process also has a positive implication. Glycerol-based denitrification was three times more efficient than methanol (Lu et al., 2010). When glycerol was added in denitrification tank, denitrification efficiency increased by 2.0 to 5.0 mg NO_3-N per 100 L of glycerol (Bodik et al., 2009). Glycerol, when used as a sole carbon source, increased the nitrogen removal in the range of 75.9 to 99.9 % to landfill leachate (Meldis et al., 2009). In industrial wastewater treatment, by increasing glycerol content from C/N 3 to 5, nitrate reduction was accomplished at 44 mg N/g.d biomass (Cyplik et al., 2013).

1.2 Project Objective

This thesis focuses on the effect of pure glycerol on readily biodegradable waste using oxygen utilization rate (OUR). The main objective of the study is to evaluate the effect of glycerol as an external carbon on readily biodegradable oxygen demand (RBCOD) for carbon limited wastewater. This research:

- Demonstrates the relationship between the RBCOD and total COD from the addition of glycerol to raw wastewater
- Illustrates the correlation of glycerol with OUR by microbial metabolism.
- Demonstrates volatile fatty acid (VFA) measurements by the addition of glycerol.

CHAPTER 2: LITERATURE REVIEW

2.1 RBCOD:-TP vs. VFA:-TP in EBPR

The wastewater organic matter in terms of total COD is divided into biodegradable, unbiodegradable and heterotrophic active mass (Wentzel et al., 1995). The biodegradable COD is further divided into readily biodegradable COD (RBCOD) and slowly biodegradable COD (SBCOD). The influent biodegradable substrate is separated into ordinary heterotrophic organisms (OHOs) and phosphate accumulating organisms (PHAs) (Wentzel et al., 1990). The steady state model is used to calculate the total use of influent RBCOD. In Biological nutrient removal activated sludge (BNRAS), influent RBCOD enters the anaerobic zone, and ordinary heterotrophic organisms (OHO) for the formation of VFAs act upon fermentable RBCOD. Another function in the anaerobic zone is the uptake of VFAs by the polyphosphate accumulating organisms (PAO) and stored as polyhdroxyalkanoates (PHAs) (Hu et al., 2002).

A study recommends the RBCOD value to be more than 25 mg/L in anaerobic zone for EBPR process with nitrification and denitrification (Sperandio et al., 2000). In an anaerobic zone, RBCOD is followed by the fermentation process to form VFA and stored within the cell as PHAs, which are subsequently consumed in the aerobic and anoxic zone (Ekama et al., 1983). The minimum required ratio of RBCOD/P for achieving the soluble effluent P less than 0.5 mg/L in EBPR is 18:1 and for VFA/P is 8:1 (Metcalf et al., 2013). The total VFA essential for phosphorus removal is reported as 4 to 16 mg per mg phosphorus (Randall et al., 1992). Barnard et al. (2006) assumed that there would be less significance of VFA if all of the RBCOD were converted into VFA in the anaerobic zone. However, the presence of high VFA in influent waste points out the

process of ongoing fermentation. In most wastewater treatment plants, 80% of influent wastewater is comprises RBCOD in the anaerobic zone.

Different studies have suggested different values for RBCOD and VFA ratio with phosphorus. The flocculation filtration method is commonly used to determine the difference between COD concentration from the influent and effluent to find RBCOD concentration (Mamais et al., 1993). The research recommended a minimum ratio of 8 to 10 g/g for RBCOD/P in the acetate fed SBR EBPR (Schuler et al., 2003). Gu et al. (2008) illustrated that the EBPR process with high RBCOD would have more phosphorus removal and presented the ratio of 5 to 38 mg RBCOD/mg P for the effluent phosphorus less than 1 mg/L. The proportion of VFA to phosphorus is commonly found in the ranges of 4 to 16 (Barnard et al., 2006). A study by Janssen et al. (1996) demonstrated that 10 g of readily biodegradable carbon was required to remove 1 g of phosphorus. Yuan et al. (2011) also reported a similar result.

2.2 RBCOD for Denitrification

In municipal wastewater, readily biodegradable substrate constitutes about 10 to 30 % and slowly biodegradable substrate about 40 to 60% of the total COD (Drewnowski et al., 2014). In the biodegradable substrate, nitrogen removal is mainly related to readily biodegradable substrate by microorganism than the slowly biodegradable substrate. The available RBCOD is essential for the wastewater plant where the influent waste has low-carbon content (Yuan et al., 2011).

If the available organic content is limited, competition for the substrate can occur between the denitrifying bacteria and polyphosphate accumulating organism (PAO). In such conditions, the extra carbon source is required to support the low concentration of influent carbon. For denitrification, the commonly used carbon sources are methanol, ethanol, glucose and acetic acid which were added to the anoxic zone of single sludge system. In denitrification, more readily degradable compounds drive the higher kinetic rate. RBCOD has electron donating capacity and contributes to the high denitrification rate. Therefore, the correct estimation of RBCOD is essential to measure nitrogen removal in the system. The denitrification potential of RBCOD can be calculated by assuming the entire fraction is used (Eq. 1) (Henz., et al, 2008):

$$\mathbf{D_{p/RBCOD} = f_{sb's}\, S_{bs}\,(1\text{-}f_{cv}Y_{HV})/2.86} \quad \textbf{(mg } \mathbf{NO_3\text{-}N/L)} \qquad \textbf{(1)}$$

Where,

$D_{p/RBCOD}$: denitrification potential of the influent RBCOD in primary anoxic reactor

S_{bs} : influent biodegradable COD (mg COD/L)

$f_{sb´s}$: RBCOD fraction of S_{bs}

Y_{HV} : OHO yield (0.45 mg VSS/ mg COD)

2.86 : Oxygen equivalent of nitrate

In aerobic condition, autotrophic nitrifying bacteria cause the oxidation of ammonium to nitrate in conventional biological process of nitrogen removal. Anoxic zone heterotrophic denitrifying bacteria convert the nitrate to nitrogen (Kuai et al., 1999). Ekama et al. (1979) hypothesized that the first part of denitrification was related to RBCOD and the second phase to SBCOD in anoxic phase. When PHA stored was lost in anoxic zone, denitrification had to rely on the rest of the available substrate, which was slowly biodegradable (SB) COD.

A study by Clayton et al. (1991) illustrated the use of RBCOD for two purposes. First in the anaerobic reactor by poly P organism and second in the primary anoxic zone for denitrification with the hypothesis of using all RBCOD by poly P organism and non poly P organism in the anoxic system. RBCOD is the small molecules, which can pass easily through the cell wall and used for the metabolism of organisms (Wentzel et al., 1992). The rate of specific growth is calculated according to the Monod equation by active mass. However, SBCOD is a complex compound and hydrolyzed to RBCOD.

The influent readily biodegradable substrate enters the anoxic zone and is consumed by the ordinary heterotrophic organism for the nitrogen removal in nitrification-denitrification activated sludge (NDAS) systems (Hu et al., 2002). RBCOD behaves as an electron donor. The presence of

low RBCOD delays nitrite reduction during anoxic operation (Uprety et al., 2013). Thus, once the level of RBCOD decreases, the rate of denitrification also depletes and relies on the compound particulate material (Naidoo et al., 2000).

Gong et al. (2013) reported that by using a ratio of 2.5:1.0 for the RBCOD to nitrate (RBCOD: NO_3^-), the ideal condition of 71.7 % of the nitrite accumulation ratio (NAR) was obtained for acetate feast-famine condition. According to Sheping et al. (2006), in the anoxic zone, the wastewater with the high fraction of RBCOD would have the highest rate of denitrification.

2.3 Biodiesel

Biodiesel is the renewable source of energy and used as the substitute for petroleum and gasoline to improve the emission of pollutants. Biodiesel is produced from vegetable oil or animal fats. One problem with vegetable oil is its high viscosity compared to the diesel engine and need to be reduced before use as alternative fuel (Demirbas et al., 2009). Transesterification is one of the general terms used to describe the process of conversion of oil to the ester (biodiesel) which is also known as alcoholysis. In transesterification, the reaction of triglycerides occurs with alcohol to form esters and byproducts called glycerol, as shown in Figure 2.1. This is a reversible reaction, and the excess amount of alcohol is used to accelerate the reaction in the forward direction (Schuchard et al., 1998). The catalyst is used to increase the product, rate and the efficiency of the reaction. The commonly used catalysts are sodium or potassium hydroxide.

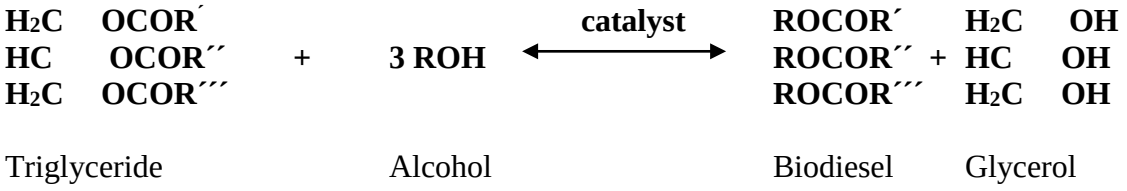

Figure 2.1: Transesterification for Vegetative Oil.

One of the standard methods of producing biodiesel is by using the triglyceride and methanol. Methanol is the commonly used because of its high economic value and easy availability. It produces the long chain fatty acid of methyl esters in the presence of strong acid or base as a catalyst. Strong acid can donate the proton to a carbonyl group whereas a base can remove the proton from alcohol. The reaction mechanism occurs in three steps. The byproducts formed are diglyceride, monoglyceride, and glycerol in first, second, and third stages, respectively. Figure

2.2 shows that from 1 triglyceride, 3 molecules of methyl ester and 1 mole of glycerol can be produced in the presence of 3 moles of alcohol. Other factors that affect the production of biodiesel are temperature, water content, pressure, molar ratio and free fatty acid content (Schuchard et al., 1998*).*

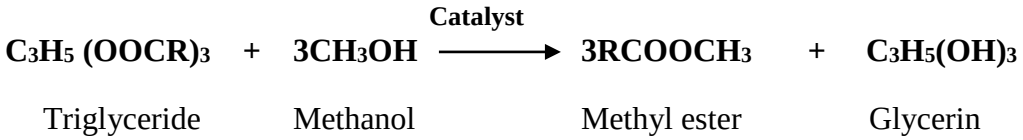

Figure 2.2: Biodiesel Production by Interesterification of Methyl-acetate.

Glycerol (glycerin) is the byproduct of biodiesel production. It is denser than biodiesel and sinks at the bottom and collects as contaminate. It occupies an average 10 % weight of the total vegetable oil. The glycerol and other contaminants in biodiesel have to be removed before using in diesel engines. Biodiesel has to undergo a number of standard tests to be used for commercial purpose. Biodiesel had renewable constituents like glycerin and used as soap by the reaction of glycerin and strong base. Methanol can also be recovered from the biodiesel or glycerin and reused.

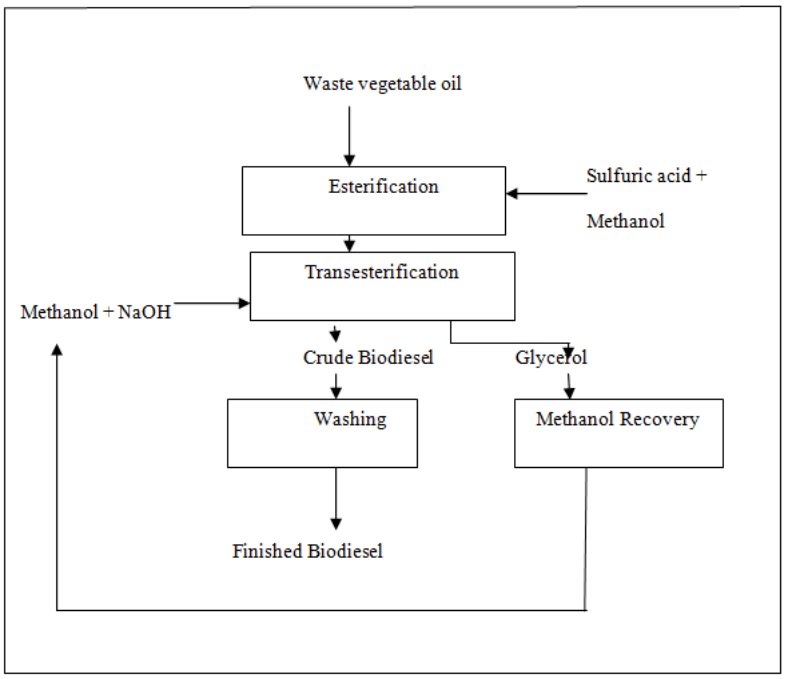

Source: Popescu et al. (2011)

Figure 2.3: Basic Technology for Biodiesel Formation.

The process can be further illustrated by taking the example of methyl ester production. The catalyst sodium hydroxide is mixed with methanol first and adequately dissolved, as in Figure 2.3. Then the oil is transferred to the biodiesel reactor and mixed with catalyst/methanol. The color of oil from light gold color turns brown within the first 20 seconds and the process of mixing continues for 8 to 10 minutes. Within a few hours, a separation between the glycerol and biodiesel will be visible. However, this glycerol will have high biodiesel content. If the entire mixture settles overnight, glycerol will stay in the bottom and biodiesel will separate on top. Glycerol is used to manufacture different products, and cleaned and filtered methyl ester (biodiesel) is directly used as a fuel for the automobiles.

2.4 Glycerol

The name glycerol has originated from the Greek word “sweet” and known as glycerin or glycerin or 1,2,3-propanetriol. Glycerol is the simplest derivative compound of propane with a trihydric alcohol. Its chemical formula is $C_3H_8O_3$ (Figure 2.4) with Molecular weight: 92.09 and found in the state of 70 to 80 % pure. Under normal conditions, the melting point is 18.2 ^{o}C, and boiling point is 290 ^{o}C with specific gravity 1.261 gm/L. Glycerol is soluble in water and alcohol, slightly soluble in ether and dioxane and insoluble in hydrocarbon (Pagliaro et al., 2008*)*. It is colorless, odorless, neutral, viscous and hygroscopic in nature.

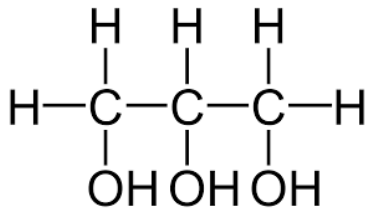

Figure 2.4: Structure of Glycerol.

Glycerol has two primaries and one secondary hydroxyl which are very reactive and can be replaceable by acid, metal, alkyl and aryl radicals to form esters, glyceroxides, and ethers, respectively. On oxidation, glycerol can produce eleven products with the original three-carbon chain by either the direct method or indirect methods. The strong oxidizing agent oxidizes the glycerol to form CO_2 and water whereas the mild oxidizing agent oxidizes only one hydroxyl group to form glyceraldehydes. Glycerol is easily reduced in the temperature above 150 ^{o}C (pressure 10 to 100 atm) with hydrogen to form 1,2-dihydroxypropane (propylene glycol) in the

presence of the catalyst. Glycerol is also reduced to isopropyl iodide when heated to 135 ^{o}C to 140 ^{o} C in the excess of hydroiodic acid.

The medium concentration of glycerol can be used as a carbon source for many organisms, either by active transport or passive transport during aerobic and anaerobic condition (Viana et al., 2012). There are two ways of the metabolic pathways for the anaerobic fermentation of glycerol (Yazdani et al., 2007). The first is the oxidative pathways where dehydrogenating of glycerol occurs by the NAD-linked glycerol dehydrogenase to form dihydroxyacetone. This is phosphorylated by the enzyme dihydroxyacetone kinase to form the various product like succinate, propionate, pyruvate, oxaloacetate, and malate as in Figure 2.5. The formation of a product depends on the environmental factors like temperature, alkalinity, pH, mixing and SRT.

In the second reductive method, glycerol was dehydrated to form 3-hydroxypropionaldehyde by coenzyme glycerol dehydratase which further reduced to 1,3-propanediol by a 1,3-propanediol dehydrogenase. The first principal product of glycerol 1,3-propanediol from fermentation was observed by Werkman et al. (1932). The formation of 1,3-propanediol from glycerol had been studied for several bacteria like *Clostridium butyricum* (Papanikolaou et al., 2004), *Paenibacillus macerans* (Gupta et al., 2009), *Escherichi coli* (Dharmadi et al., 2006; Chaudhary et al., 2010), *Propionibacterium freudenreichii* ssp. *Shermanii* (Kosmider et al., 2010), *Citrobacter freundii* and *Hafnia alvei* (Drozdzynska et al., 2014).

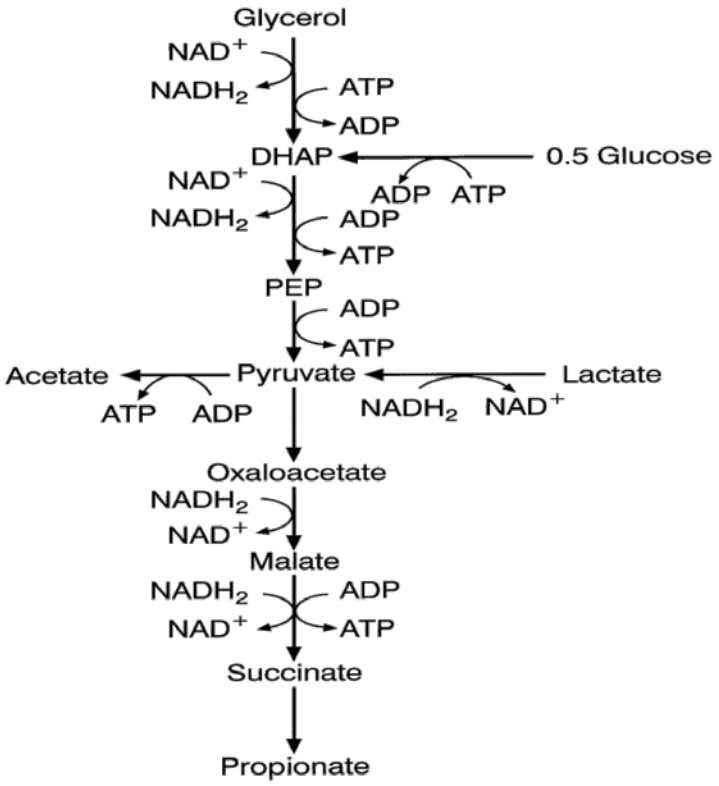

Source: Barbirato et al. (1999)

Figure 2.5: Propionic Acid Fermentation Pathway From Glycerol.

A study by Sattayasamitsathit et al. (2011) stated *Klebsiella pneumoniae* bacteria for the batch fermentation of 40 to 100 g/L crude glycerol with the pH range from 6.5 to 7.5 and temperature between 31 to 40 ^{o}C to study two-phase pH controlled strategy. The best result was achieved with most production of 24.0 g/L 1,3-propanediol with the productivity of 1.78 g/L.hr during the incubation period of 16 hours with the feeding rate of 0.1 L/h. Chaudhary et al. (2011) reported *Escherichia coli* K-12 for the fermentation of glycerol in ethanol, hydrogen and cell growth in full plant design with three replicates. The maximum hydrogen production (32.15mmol/L) and ethanol production (0.40 g/g glycerol) were achieved in 25 g/L and 10 g/L

glycerol concentration, respectively. The experiment also showed the negative effects of hydrogen production on the cell growth.

In wastewater, fermentation of glycerol to a simpler form (volatile fatty acid) like acetate, propionate, or succinate is essential for the ideal use by the microorganism. The production of propionic acid is associated with the Gram-positive *Propionibacterium* genera which are capable of utilizing glycerol during the fermentation process (Clomburg et al., 2013). *Propionibacterium acidipropionic* could produce 46 g/L propionic acid from 80 g/L glycerol with the productivity of 0.36 g/L.hr. Barbirato et al. (1997) tested the *Propionibacterium acidipropionic, Propionibacterium acnes* and *Clostridium propionicum* for the conversion of 20 g/L glycerol to propionic acid during the batch fermentation. *Propionibacterium acidipropionic* showed the high efficiency compared to the other two species regarding production. Propionic acid generation from glycerol was compared with other carbon sources such as glucose and lactic acid. The total productivity of propionic acid was 0.18 g/L.hr by glycerol whereas, the conversion decreased by 17 % and 13% while using glucose and lactic acid, respectively. Himmi et al. (2000) also focused on the fermentation of propionic acid by using *Propionibacterium acidipropionic, Propionibacterium freuenreichii* ssp. and *Shermani* with two carbon sources as glycerol and glucose in an aerobic batch reactor. The study showed that in 20 g/L glycerol or glucose, the primary end product was propionic acid followed by acetic acid, n-propanol, and succinic acid. *Propionibacterium acidipropionic* had greater efficiency with the production of 0.42 g/L.hr (0.79 mol/mol) propionic acid. Similarly, in another review of 20 g/L glycerol by *Propionibacterium acidipropionic* and *Propionibacterium freuenreichii* ssp., *Shermani*, the production of propionic acid were 0.79 and 0.58 mol/mol, respectively (Bories et al., 2003).

2.5 Impact of Glycerol in EBPR

Enhanced biological phosphorus removal (EBPR) lowers the phosphorus level without using chemical through activated sludge process (Oehmen et al., 2007). The group of microorganism responsible for phosphorus removal is polyphosphate accumulating organisms (PAOs). These organisms are capable of storing the phosphate as intracellular polyphosphate. Under anaerobic condition, polyphosphate is used to generate energy to transport volatile fatty acid (VFAs) into the cell and store them into Poly-β-hydroxyalkanoates (PHAs). VFAs, which need reducing equivalents for biotransformation into PHAs, are supplied through the glycolysis of the glycogen. The anaerobic condition is favorable for the growth of PHAs by decreasing the amount of polyphosphate and glycogen. In aerobic condition, PHA oxidizes in the presence of oxygen by producing energy and storing in newly form polyphosphate. Aerobic condition favors the formation of glycogen and polyphosphate thus decreasing the formation of PHAs. Some of the PHA carbons are also transforming into glycogen. Glycogen accumulating organism (GAOs) uses the glycogen for energy and converts into PHAs. In an anaerobic condition, some of the GAOs compete with PAOs for the substrate like VFAs and sugars.

EBPR is commonly used for the removal of phosphorus in wastewater treatment. The GAO and PAO are the two dominant organisms for EBPR. PAO is capable of storing the phosphorus as polyphosphate and hence contributes to the phosphorus removal by releasing orthophosphate in the solution. GAO uses the VFAs and does not contribute to removing phosphorus. One of the main reasons for the failure of EBPR can be the superfluous growth of GAO over PAO and GAO competition for biomass substrate over PAO (Oehmen et al., 2006).

Therefore, the favorable environment for PAO helps to improve EBPR process. Acetate and propionate are commonly used as a carbon substrate for phosphorus removal in EPBR. Acetate provides the convenient adaptability to polyphosphate accumulating organism under anaerobic and aerobic conditions to synthesize the intracellular storage compound. PHA products were mainly poly-hydroxy-butyrate (PHB) and poly-hydroxy-valerate (PHV) when using acetate and propionate, respectively (Randall et al., 2002). When acetate and propionate were used as the carbon source, anaerobic P release is less in propionate, whereas aerobic P uptake and anaerobic VFA uptake were similar in both cases (Pijuan et al., 2004).

Several researchers have investigated glycerol as a carbon source in EBPR. Glycerol was fermented with waste activated sludge to study its impact on biological phosphorus removal (Yuan et al., 2010). The waste activated sludge from the reactor was replaced by the same amount of glycerol to increase the production of volatile fatty acids (VFA). The results showed the significant amount of VFAs with propionic acid as the primary end product. This enhanced the EBPR without causing the adverse impact on denitrification.

The low-level of organic content in influent wastewater results in the failure of EBPR in full-scale plant. In such situations, an external carbon source is necessary to get the desired level of phosphorus removal. A study of Guerrero et al. (2012) highlighted the use of glycerol for two different strategies. In the first case, glycerol was directly used as a sole carbon source and the second instance involved the two types of association between glycerol anaerobic degraders and PAO. The result was favorable in longer anaerobic phase for glycerol as a sole carbon source. A

longer anaerobic phase also favored the degradation of anaerobic glycerol to PAO due to the availability of high sludge. The proper configurations obtained were 4h and 3.5h for anaerobic and aerobic, respectively as a single carbon source. This research for the first time showed the feasibility of glycerol in the single sludge configuration.

Crude glycerol is considered as an alternative carbon source. Long chain fatty acid (LCFA), one of the glycerol parameters, was studied to find the effect on PAO (Taya et al., 2015*)*. The study focused on the effect of LCFA for short-term and long-term exposure. The results showed that excess use of glycerol decreased PAO activity by adsorption on the surface of microorganisms. The short-term study was able to sustain the PAO activity. However, a long-term exposure created operational problems by increased biomass.

Coats et al. (2015) focused on the different aspects than anaerobic phosphorus release for successful EBPR by using crude glycerol. The study illustrated the carbon cycle by PAOs anaerobically to generate ATP energy for VFA uptake. PAO only consumed poly P reserves if the substrate energy was low for metabolism.

2.6 Impact of Glycerol in Denitrification

Nitrogen and phosphorus are removed from wastewater in tertiary treatment before disposal. The important chemical species in wastewater are ammonia, nitrate, nitrite, and nitrogen. Nitrification is the process of removing ammonia (NH_4^+) in two steps first oxidizes to nitrite (NO_2^-) and second to nitrate (NO_3^-) by ammonia oxidizing bacteria (AOB) and nitrite oxidizing bacteria (NOB), respectively. Aerobic autotrophic chemolithotrophs especially Nitrosomonas and Nitrobacter bacteria are responsible for nitrification. Nitrification is carried out as (Eq. 2 to 6):

First Step:

$$\mathbf{2\ NH_4^+ + 3O_2 \longrightarrow 2\ NO_2^- + 4\ H^+ + 2\ H_2O} \qquad \mathbf{(2)}$$

Second Step:

$$\mathbf{2\ NO_2^- + O_2 \longrightarrow 2NO_3^-} \qquad \mathbf{(3)}$$

Net Reaction:

$$\mathbf{NH_4^+ + 2\ O_2 \longrightarrow NO_3 + 2\ H^+ + H_2O} \qquad \mathbf{(4)}$$

Nitrification also consumes alkalinity. Half of alkalinity consumed in nitrification is recovered in denitrification process. Denitrification is performed by facultative aerobic heterotrophic chemoorganotrophs by converting nitrate into nitrogen (N_2) through a series of intermediate product (nitric oxide (NO), nitrous oxide (N_2O)).

$$\mathbf{NO_3^- \longrightarrow NO_2^- \longrightarrow NO + N_2O \longrightarrow N_2\,(g)} \qquad \mathbf{(5)}$$

The overall reaction:

$$\mathbf{2\ NO_3^- + 10e^- + 12\ H^+ \longrightarrow N_2 + 6\ H_2\ O} \qquad \mathbf{(6)}$$

Organic matter is also essential for denitrification. Denitrification is commonly used in wastewater to remove nitrogen. The Modified Ludzack- Ettinger (MLE) process is a common biological process for the nitrogen removal (Uprety et al., 2012). In biological nutrient removal (BNR), it is necessary to keep nitrate out of the anaerobic zone to have nitrification and denitrification for stable phosphorous removal. The partial denitrification can cause breaking of nitrite and nitrate in the aerobic zone and filamentous bulking as well. The presence of nitrite reduces denitrifying phosphate uptake both in the aerobic and anoxic zone. It provides the favorable environment for GAO and competes with PAO in anaerobic zone (Saito et al., 2004).

The denitrifying bacteria compete with PAO for the metabolic substrate and inhibit the release of anaerobic phosphorus and EBPR activity. Denitrification rate depends on the nature and availability of biodegradable organics. It also depends on the environmental condition like pH, temperature, dissolved oxygen, and presence of carbon and nitrite (Foglar et al., 2003). There are two types of PAO recognized: denitrifying PAO and denitrifying Poly P accumulating organisms (DNPAO) (Seviour et al., 2003). PAOs have a lower endogenous decay coefficient. In order to protect from the breakpoint, the anoxic zone is designed to prevent the nitrate from anaerobic zone for complete denitrification by proper use of COD/N and internal recycle ratio. Wastewaters with high COD/N ratio need to have high recycled ratio or post-denitrification to remove the total nitrogen (Lee et al., 2001).

In order to meet the nitrogen limit, additional carbon source as electron donor has to be added in BNR process. In the past decade, different carbon sources have studied to find the

effectiveness and improvement in N removal. The commonly used carbon sources for the study are methanol, acetic acid, benzoic acid and glucose. A research work of Her et al. (1995) signified aromatic (benzoic) compound with less denitrification efficiency than non-aromatic compound under a constant C/N ratio. For non-aromatic (methanol, acetic acid, and glucose) compounds, efficiency depended on the molecular weight and chemical structure and required minimum C/N ratio. Among non-aromatic compounds, the requirement for the minimum C/N ratio depended on the molecular weight and increased with weight.

When the complex compound (sucrose) was used as the carbon source, enhanced biological phosphorus removal process failed (Guerrero et al., 2012). The presence of nitrite inhibited the fermentation process for VFA production and caused the failure of phosphorus removal. The carbon source with a lower molecular weight was easily degradable and allowed high denitrification rate.

A limited supply of carbon results in the intermediate nitrites species whereas; the extra supply caused the carbon breakthrough. It is also important to select the appropriate carbon source for the BNR. Cost-effective and low chain carbon source results in less sludge and efficient denitrification (Uprety et al., 2013). The research studied the effect of methanol, pure glycerol and biodiesel glycerol waste in three sequencing batch reactors. The high amount of carbon resulted in the small nitrogen residual. However, low dose only removed the partial TN in all three reactors. Glycerol reactor had high nitrite accumulation than the methanol.

In a study by Hinojosa et al. (2008), biodiesel byproduct glycerol was added during the denitrification process to study denitrification rate, C: N ratio and maximum growth rate in the batch experiments. The study showed the minimum C/N ratio calculated as 4.2 mg COD/mg NOx-N with the maximum growth rate of 3.4/d. Another study on glycerol evaluated the effectiveness in a landfill by Melidis et al. (2009). The study analyzed the results from the use of carbon and without carbon for the nitrogen compound removal. When there was no carbon source, N removal was insignificant, and there was an accumulation of nitrate and nitrite. However, with the use of glycerol as a carbon source the nitrogen removal improved in the range of 75.9 % to 99.9 %.

In the study of constructed wetland, use of glucose as a carbon source increased the nitrate removal of 30 to 40 mg/L nitrate. In summer, the removal increased from 20 % to more than 50 % and in winter increased from 10 % to 30 % with the retention time of 24 hour (Songliu et al., 2009). However, more supply of carbon source in summer and winter increased the acclimation of nitrogen from 0.15 mg/ L to 2 mg/L in the effluent.

Glycerol was studied to find the appropriate C/N ratio for complete removal of nitrate without activating the anaerobic glycerol metabolic pathway of denitrification. The C/N ratio of 3 was considered as the best practice with the entire removal of nitrates with the formation of 0.16 g/L 1, 3-propanediol and 0.11 g/L acetic acid (Cyplik et al., 2013). In another study, the C/N ratio of 2 showed a higher N_2O in the gass phase than C/N ratio of 3 to 4 causing incomplete nitrite removal (Katarzyna et al., 2015). Denitrification was found efficient in C/N ratio between 2.5 to 4.0 with an optimal ratio of 3 for glycerin.

CHAPTER 3: MATERIALS AND METHODS

The influent wastewater was collected from the Iron Bridge Wastewater Reclamation Facility (Oviedo, FL) and stored in the walk-in cooler at 4 ^{o}C. The samples were gathered during the period of September-December 2015. The average values were calculated from 7 data samples between study periods (Table 3.1). The Iron Bride Facility is designed to protect the local surface waterway in Central Florida environment and provide service to the cities of Orlando, Winter Park, Maitland and other neighboring communities.

Table 3.1: Characteristics of the Wastewater

Influent Wastewater	pH	TCOD (mg COD/L)	VFA (mg COD/L)	TP (mg P/L)	TN (mg N/L)	RBCOD (mgCOD/L)
Average Value	7.4	276	3.0	4.6	35.6	59.0
Standard Deviation	0.2	43.0	8.0	1.3	0.4	18.4

Table 3.2 represents the methods and equipment used for the experiments. RBCOD was measured by the respirometry method (Randall et al., 1999). During the study period, two set of RBCOD apparatus were operated in the laboratory of University of Central Florida (UCF). Pure glycerol (Fisher Scientific, G33-1) of density 3.17 was used to prepare the stock solution. 6.67 g of pure glycerol was added to 1-L of DI. The glycerol stock solution was stored in the laboratory.

Table 3.2: List of Methods and Equipment for RBCOD Study

Test	Test Location	Method/ Equipment Description	Measuring Unit
RBCOD	UCF Laboratory	Respirometry Method/ Hitech MicroSystem, Capetown, South Africa	mg COD/L
Glycerol	UCF Laboratory	Spectrophotometric Method/ HACH 4940 CF 124035	mg/L
VFA	UCF Laboratory	Gas Chromatography/ model 14-A, Shimadzu	mg COD/L

The effect of glycerol on RBCOD was studied in three different phases. In first and second phase, 30 mL and 15 mL glycerol stock solution were added to two-liter wastewater sample, respectively at time zero. The experiments were allowed for twenty-four hours and data were analyzed. In phase II, a time series for glycerol and VFA were performed. The first sample was taken at time zero and rest at the interval of two hours with eight samples altogether. All the samples were measured next day to get the readings. The glycerol was measured by the Spectrophotometric method (Bondioli et al., 2005) and VFA by using Gas Chromatography (14-A, Shimadzu).

In the third phase, 5 mL inoculate, and 30 mL glycerol stock solutions were added to the 2-liter wastewater. 5 mL inoculate was taken from the glycerol acclimated prefermenter managed by another colleague in University of Central Florida Laboratory. The prefermenter had 1,500 mL of primary solids with a solid retention time (SRT) and hydraulic retention time (HRT) of 4 days. Every day 375 mL of primary effluent was removed and refilled with 6,500 mg pure glycerol plus 375mL new primary solids and wastewater in 1:1 ratio to maintain a constant

volume in the prefermenter. The prefermenter was operated to remove the significant amount of glycerol. The mixed liquor suspended solid (MLSS) of glycerol acclimated biomass was measured as 5,500 mg/L with the VSS/TSS ratio of 0.88. The main reason to add acclimated glycerol sludge was to see the effect on the wastewater.

3.1 OUR Calibration

3.1.1 Main Knob for Calibration

Once the DO/OUR Meter (IP55-685.008, Hitech Micro Systems, Capetown, South Africa) was turned on, temperature and DO (mg/L) displayed on the front panel. F key was pressed to change the operation mode (Mode A). Sodium sulphite solution of 100 mg in 100 mL DI water was prepared. Every time the solution was freshly made and used within 30 minutes. The DO probe (YSI, 5739) and the wire thermometer (Mylar Screened Cable, 0.22mm) were placed in the sodium sulphite solution and suspended 1 inch above the bottom and allowed for 1 min to get the stable reading. The Main knob (Zero knob) located on the left side of the unit was adjusted such that the DO was less than or equal to 0.5 mg/L. Once it was calibrated, the DO probe and wire thermometer were removed from the solution and rinsed with DI water. In order to verify the zero setting, the DO probe and wire thermometer were placed in sodium sulphite solution again to get the reading, and the both are cleaned with DI water. The calibration of Main knob could be done twice a month or once having the peculiar results.

3.1.2 Gain knob for Calibration

A beaker was filled with 100mL DI water, and aeration stone was added. The beaker was covered with plastic wrap to limit the oxygen diffusion from surface to water. The pump button was turned on and allowed the aeration until the water was fully saturated and showed the stable DO reading. The beaker was left for 3 minutes. Once the water reached the saturated condition, the DO probe and temperature wire were placed 1 inch above the bottom. In order to calibrate,

the gain knob was adjusted to get the saturated reading for the water temperature (e.g., DO= 9 mg/L at 21 ^{o}C). The calibration of the gain knob was done manually before each experiment.

Figure 3.1: DO/OUR Meter.

3.2 Analytical Procedures

3.2.1 RBCOD

The wastewater sample (2-L) from the cooler was allowed to warm for an hour to room temperature. In OUR Meter, the upper limit, and lower limit DO were set as 6 and 4 mg/L, respectively. The wastewater sample was filled in a 2-L beaker with a stir bar and placed on the mixing plate (120S, Thermix Stirrer, Fisher Scientific). The stirring was set at the low speed to mix the sample. It was important to make sure that mixing intensity was not very high which could cause the vortex. DO probe and temperature wire were added to the sample and suspended 1 inch above the container bottom. The aeration stone was placed in the sample above 1 inch. The pump button and DO/OUR meter were changed to auto. Two mL of sample was taken from the container to measure the initial TCOD.

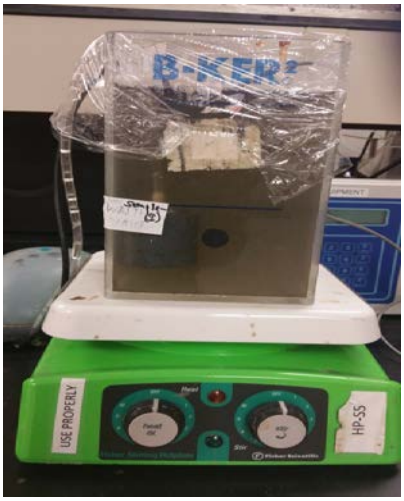

Figure 3.2: RBCOD Experiment Sample.

The beaker was covered with the plastic wrap to prevent diffusion. The computer and OUR meter were turned on when aeration would start if its value is below 4 mg/L. Aeration

continued until it reached 6 mg/L and the process continued as DO value drops. This experiment was carried out for 24 hours. The computed data for the experiment were recorded in DOMWIN software program. After 24 hours, the data were downloaded from DOMWIN to a thumb drive or any floppy disk. The probe, thermometer and aeration stone were removed from the sample container and properly cleaned with DI. The DO probe was placed back into the storage bottle and all other at the proper place. The final TCOD was measured for the sample.

3.2.2 Glycerol

A spectrophotometric method was used to determine the glycerol concentration in the wastewater samples. The working reagents of an acetic acid stock solution of 1.6M (9.6 g/100 mL) and ammonium acetate stock solution of 4.0 M (30.8 g/100 mL) were prepared. The acetylacetone solution (0.2 M) and sodium periodate solution (10mM) were also prepared. The samples were collected as 0, 0.5, 1, 1.5 and 2 mL in test tubes, and 1.2 mL of 10mM sodium periodate solution was added to the samples. In the samples, 1.2 mL of acetylacetone solution was added and stirred manually. The samples were measured with the spectrophotometer set (HACH 4940 CF 124035) in double beam mode at 410 nm.

3.2.3 VFA

Short chain volatile fatty acids (SCVFAs) were measured by the gas chromatography (model 14-A, Shimadzu) method. The samples were analyzed in the initial column temperature of 110 ^{o}C which increased with the rate of 5 ^{o}C/min until 190 ^{o}C. The 1.5 mL of samples filtered by 0.45 µm membrane filters were transferred to the GC vials and acidified with 2 µL of 3 % H_2PO_4. The samples were measured by injecting volatile free acid mix containing 10 mM SCVFAs.

3.2.4 Laboratory Quality Control

During the data analysis, duplicates and spike samples were collected to check the accuracy and consistency of the data. A duplicate sample and spike sample were measured for every two samples during the glycerol and VFA analysis. The accuracy of data for batch tests was evaluated by COD mass balance as equation 7.

$$\text{COD Recovery (\%)} = \frac{\text{COD}_{t=T} + \int_{t=0}^{t=T} \text{OUR}\, dt}{\text{COD}_{t=0}} \times 100$$

Where,

t = time (hr)

$COD_{t=T}$ = total unfiltered COD concentration at end of test (t=T) (mg COD/L)

OUR = Oxygen utilization rate (mgO_2/L.hr)

$\int_{t=0}^{t=T} \text{OUR}\, dt$ = integral area under the OUR vs. time plot between start and end of test (mgO_2/L)

= oxygen concentration consumed over the test

The industrial statistics (I statistics) as in equation 8 was used to measure the precision of the data. In an equation, A represents the sample value and B as the duplicate value.

$$I = \frac{|A-B|}{A+B} \quad \textbf{(8)}$$

CHAPTER 4: RESULTS AND DISCUSSION

Batch experiments were conducted to measure the readily biodegradable oxygen demand (RBCOD) at room temperature (25 ^{o}C) between September-December, 2015. The wastewater was collected from Iron Bridge Wastewater Reclamation Facility. Two different RBCOD sets were used to perform the batch experiments in the laboratory. The first set was for the control sample and the second set was spiked with glycerol of concentration 6.67 g/L.

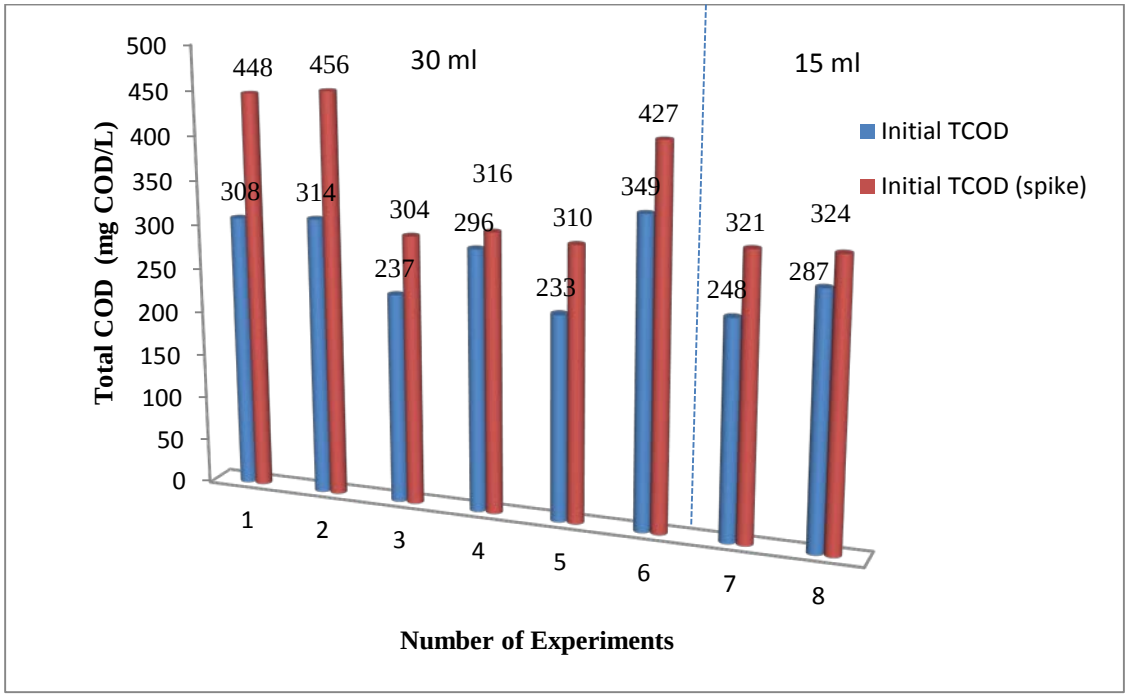

Figure 4.1: Initial TCOD of Influent Wastewater.

Average total chemical oxygen demand (TCOD) in wastewater were 284 mg COD/L and increased up to 378 mg COD/L and 323 mg COD/L for 30 mL and 15 mL glycerol concentration, respectively. Effect of glycerol on TCOD level is shown in Figure 4.1. The TCOD levels in all experiments are increased by glycerol addition.

RBCOD was determined by analyzing the time series data from oxygen utilization rate (OUR). OUR measured the oxygen consumption rate of bacteria in contact with wastewater. OUR concentration gradually increased from 2 to 5 hours, whereas, it significantly dropped after 5 hours (Figure 4.2). One of the reasons could be the reduction of readily biodegradable substrate for the microorganism.

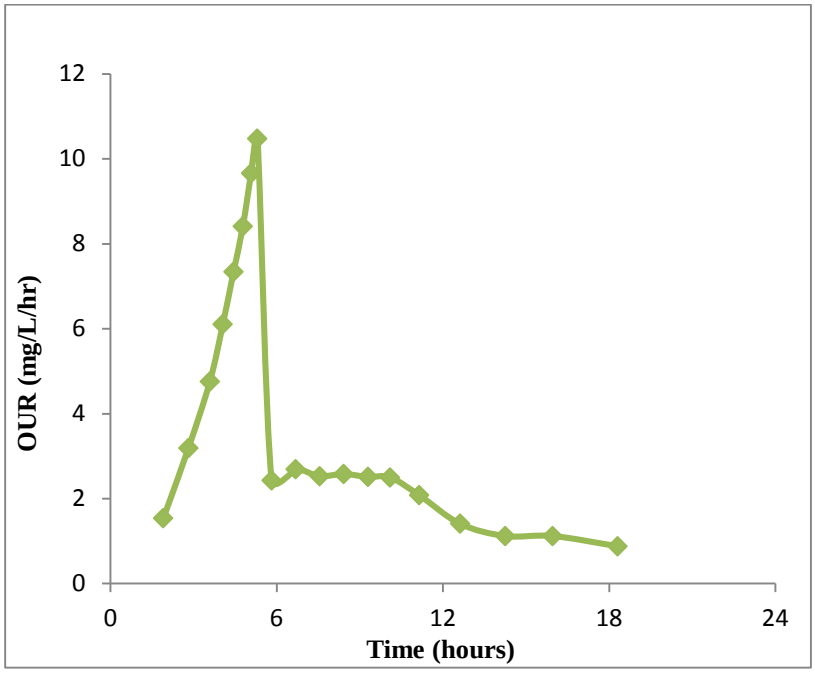

Figure 4.2: OUR Plot vs. Time

In influent wastewater, the RBCOD varied between 38 to 81 mg COD/ L (the average value 52.0 mg COD/L) and represented 12 to 28% (the average value 20 %) of total COD (Rossle et al., 2001; Orhon et al., 2002; Dauknys et al., 2009) as shown in Figure 4.3. The influent RBCOD concentration is necessary to determine the accurate effluent phosphorus and nitrate concentration. RBCOD provides the substrate for PAO to consume VFA fermentation product in anaerobic zone (Henze et al., 2008). TCOD recovery for the sampling was found approximately 71% to 78% with an average value of 73%.

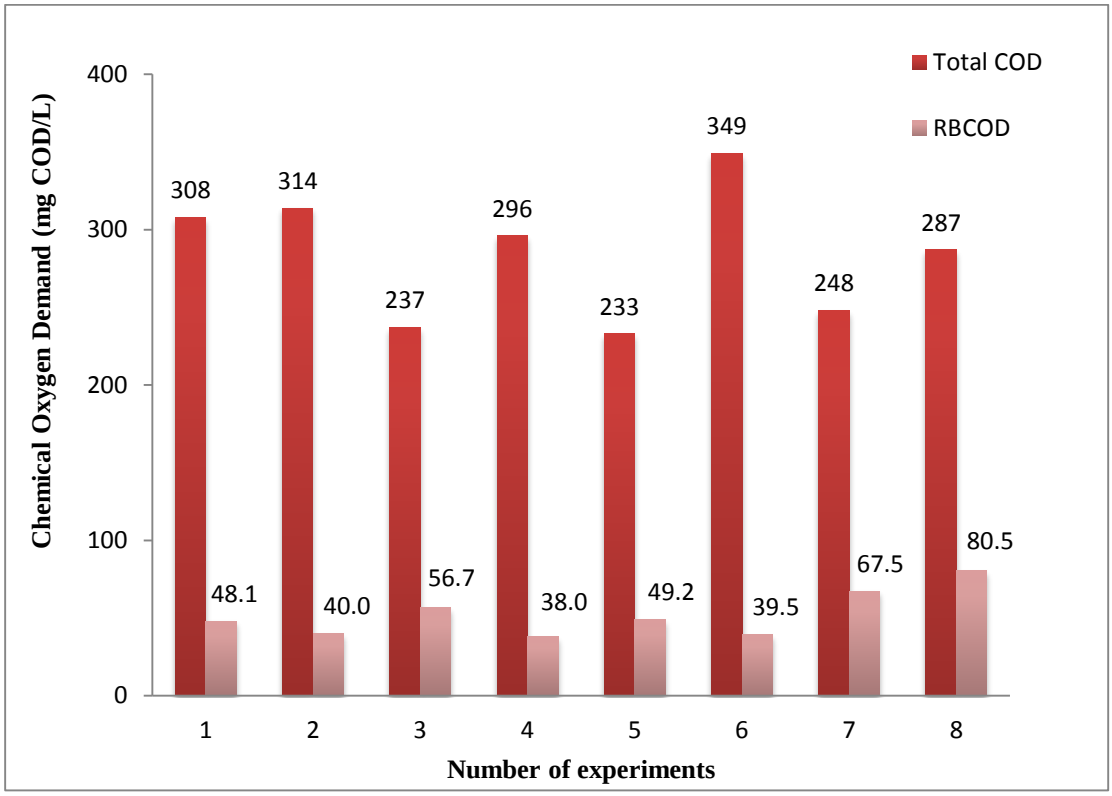

Figure 4.3: TCOD/RBCOD Trend in Wastewater

RBCOD is further divided into fermentation products (VFAs) and readily fermentable biodegradable fraction (F-RBCOD). VFAs comprise 2 to 10 % of total COD whereas fermentable RBCOD consist of 10 to 20 % of total COD (Rossle et al., 2001; Naidoo et al., 1999). In the influent wastewater, the rate of VFA uptake is very high by the microorganism for the microbial growth and reproduction (especially by PAO) and stored as polyhydroxyalkanoates (PHA) in the cells in anaerobic condition. The readily fermentable substrates are directly available to the heterotrophic microorganisms and form the substrate for the fermentation (Naidoo et al., 1999).

SBCOD represents 50 % to 77 % of TCOD (Rossle et al., 2001). SBCOD are slowly consumed and metabolized by microorganisms and represents the rate of 10 % compared to RBCOD uptake (Naidoo et al., 1999). The complex compound is broken down into the simpler molecules by the extracellular enzyme and utilized by the microorganism.

4.1 Phase I

The effect of glycerol on oxygen demand was investigated in three different stages of the study. In the first phase, the first sample had 2 liters of influent wastewater as an un-spiked sample (control sample) and the second sample has 2-liter influent wastewater plus 30 mL spike solution. The spiked sample contained 6.67 g/L of glycerol, which was added at the beginning of the experiment. The initial concentration of glycerol in wastewater was 98.5 mg/L (approximately 120 mg COD/L). Both of the experiments were conducted for 24 hours, and reading was taken the next day.

A 30 mL spike wastewater resulted in two different peaks of the OUR as shown in Figure 4.4. The presence of two carbon sources for bacteria can lead the metabolism at the same time or at different times, referred to as diauxic growth (Boulineau et al., 2013). The first peak indicated the exponential growth based on the readily biodegradable substrate and showed the same standard growth curve. RBCOD ran out, and OUR value dropped by 5 to 6 hours of operation and again increased to the second peak by ± 13 hrs. At the start of the batch, the average initial heterotrophic active biomass (Z_{BH}) for RBCOD was calculated as 5.40 mg VSS/L (8 mg COD/L) and increased up to 15.8 mg VSS/L (23.4 mg COD/L). The heterotrophic mass is the active agent whereas biodegradable fraction is regarded as the substrate (Vollertsen et al., 2002).

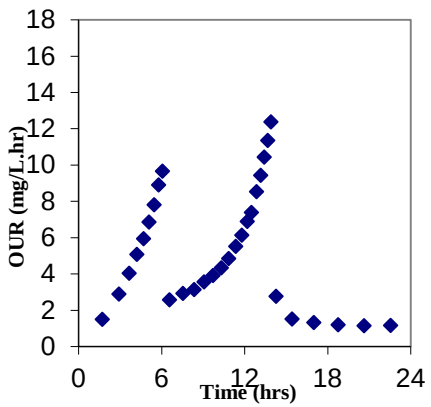

OUR graph (09/01/2015)

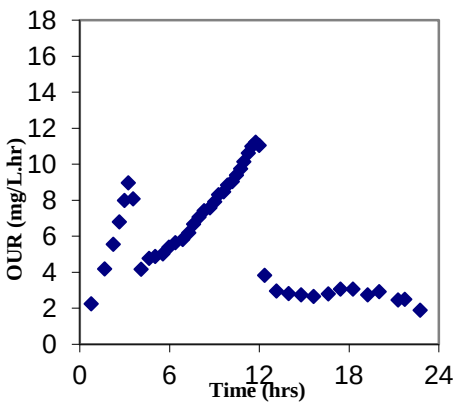

OUR graph (09/02/2015)

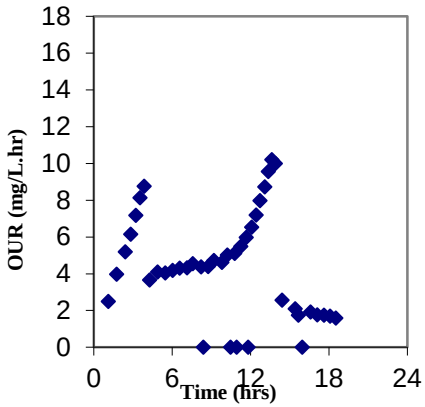

OUR graph (09/24/2015)

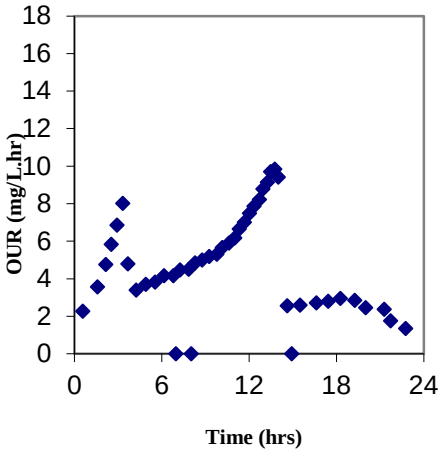

OUR graph (09/25/2015)

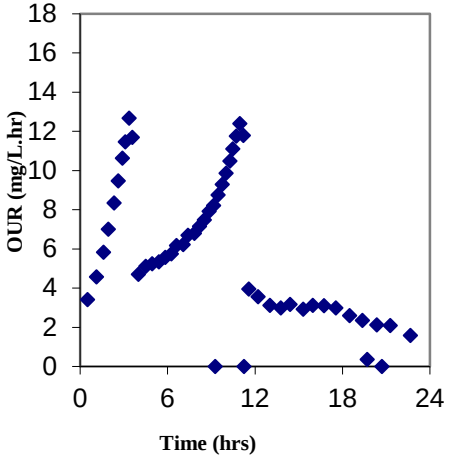

OUR graph (09/28/2015)

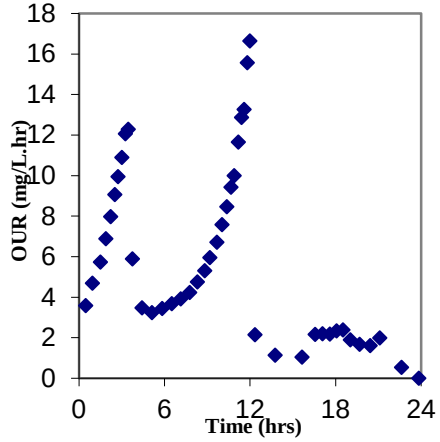

OUR graph (09/29/2015)

Figure 4.4: Effect of Glycerol on Different RBCOD Spike (30 mL) Samples.

As shown in Figure 4.4, glycerol was not acclimated by the bacteria between 5 to 6 hours. After 6 hours, the peak started to increase indicating glycerol as energy. In the second lag phase, microorganisms produced the enzymes for the consumption of glycerol as a carbon source. The average oxygen demand (from 6 data points) for the glycerol peak is 129 mg COD/L, which is slightly higher than the theoretical oxygen demand value (120 mg COD/L) with an error of 7 % (Table 4.1).

Table 4.1: Results of Phase I Statistical Data

Parameter	Un-spike Sample RBCOD(inf.) (mgCOD/L	RBCOD (P_1) (mgCOD/L)	Spike Sample RBCOD(P_2) (mgCOD/L)
Minimum Value	38.0	24.0	105
Maximum Value	56.7	58.6	143
Average Value	45.3	41.9	129
Standard Deviation	7.00	14.0	13.0

*Theoretical oxygen demand (TOD) of glycerol is 1.22 mg COD/ mg glycerol and multiply with glycerol dosage 98.5 mg/L (= 120 mg COD/L) to compare data of spike; $P_{1=}$ Peak 1, P_2= Peak 2

4.2 Phase II

In the second phase, 15 mL spike was added to the wastewater. The primary objective of this phase was to observe the kinetic effect of glycerol on oxygen demand. The initial concentration of glycerol in wastewater was approximately 50.0 mg/L, which is equal to 61.0 mg COD/L. Figure 4.5 demonstrated the same diauxic growth as in the first stage of the study. The un-spike wastewater showed similar results as those in phase I.

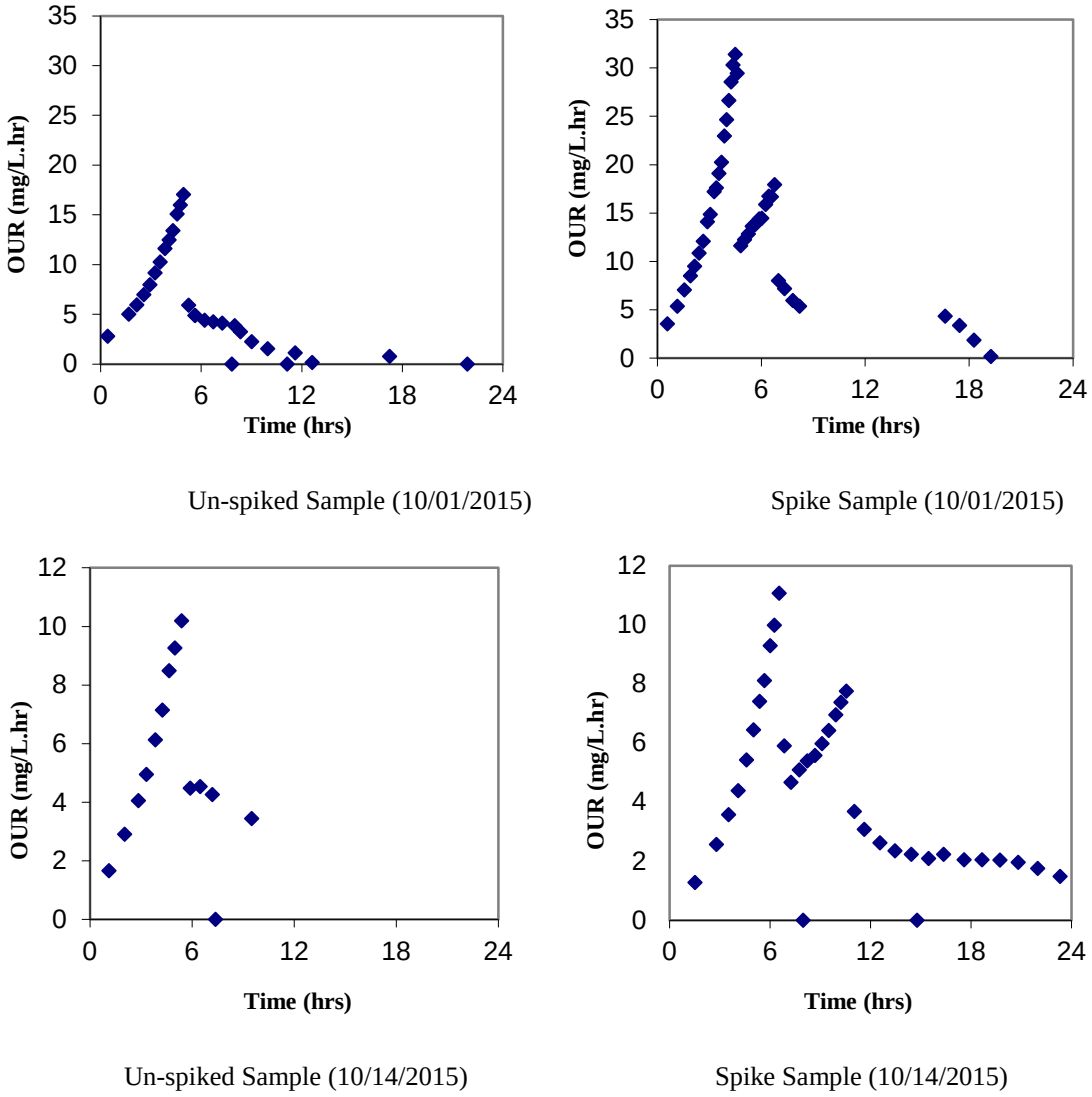

Figure 4.5: Comparison of Un-spike Sample with Spike Sample.

The reduced volume of spike solution decreased the height of OUR in the second peak as shown in Figure 4.5 B and D. This result supports that glycerol concentration was affected by the oxygen demand. This batch of experiments had a slightly higher value of RBCOD than the first stage of the study. The reason could be due to the change in the composition of influent wastewater from Iron Bridge. The average oxygen (2 data points) demand for the glycerol peak showed 86.7 mg COD/L, which is higher than the theoretical oxygen demand value (61 mg COD/L) (Table 4.2).

Table 4.2: Results of Phase II Statistical Data

Parameter	Un-spike Sample		Spike Sample
	RBCOD(inf.) (mgCOD/L	RBCOD(P_1) (mgCOD/L)	RBCOD(P_2) (mgCOD/L)
Minimum Value	67.5	55.6	66.4
Maximum Value	80.5	113	107
Average Value	74.0	84.3	86.7
Standard Deviation	9.00	40.0	29.0

*Theoretical oxygen demand (TOD) of glycerol is 1.22 mg COD/ mg glycerol and multiply with glycerol dosage 50 mg/L (= 61 mg COD/L) to compare data of spike; $P_{1=}$ Peak 1, P_2= Peak 2

4.2.1 Time Series

Glycerol and VFA time series were performed in the wastewater containing 15 mL glycerol stock solution (6.67g/L) in the second phase. The principal purpose of time series was to observe the concentration of glycerol with the change of time and its relation with the spike wastewater. The first sample was taken at the initial point of the experiment (time zero) and collected eight

samples in the interval of 2 hours altogether. The Figure 4.6 showed the trend of glycerol concentration over time. The initial concentration of glycerol in a wastewater was approximately 50 mg/L. After two hours, the amount of glycerol began to decrease with time. From the Figure 4.5 (B & D), the use of glycerol started from approximately 5 to 6 hours of operation and all the glycerol ended by about 12 hours of operation. This bar diagram verified the results from the OUR curve by representing no glycerol after 10 hours. The microorganisms metabolized all of the glycerol.

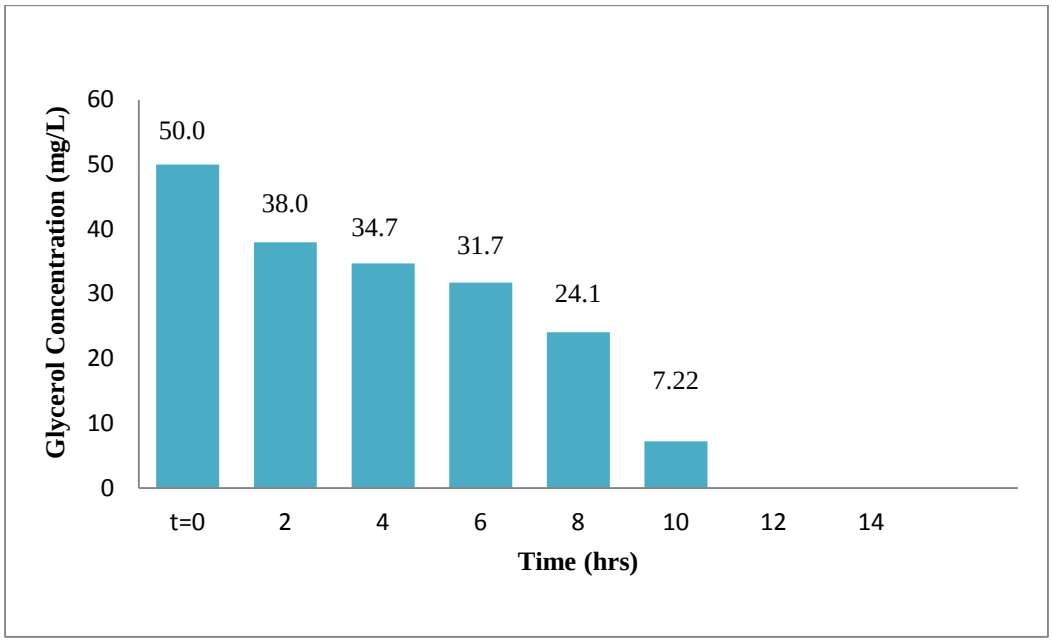

Figure 4.6: Time Series Data for Glycerol.

The VFAs of the influent at time zero was 10 mg COD/L. The microorganism utilized VFAs for the growth and reproduction represented by the increase of curve in Figure 4.5 OUR graph. Once the organism consumed all of VFA, there was no VFA in wastewater, which was indicated by the time series in Figure 4.7. Figure 4.6 and 4.7 illustrated that the microorganisms

consumed all the glycerol without formation of VFAs at the time of 12 hrs. Bacteria did not use glycerol since the bacteria had not synthesized the enzyme for the digestion of glycerol. Fermentation process starts once microorganism accumulated all the glycerol and formed the short chain volatile fatty acid, which was indicated by a peak at 14 hrs in Figure 4.7. Glycerol resulted in the high volume of VFAs with propionic acid as the primary end product.

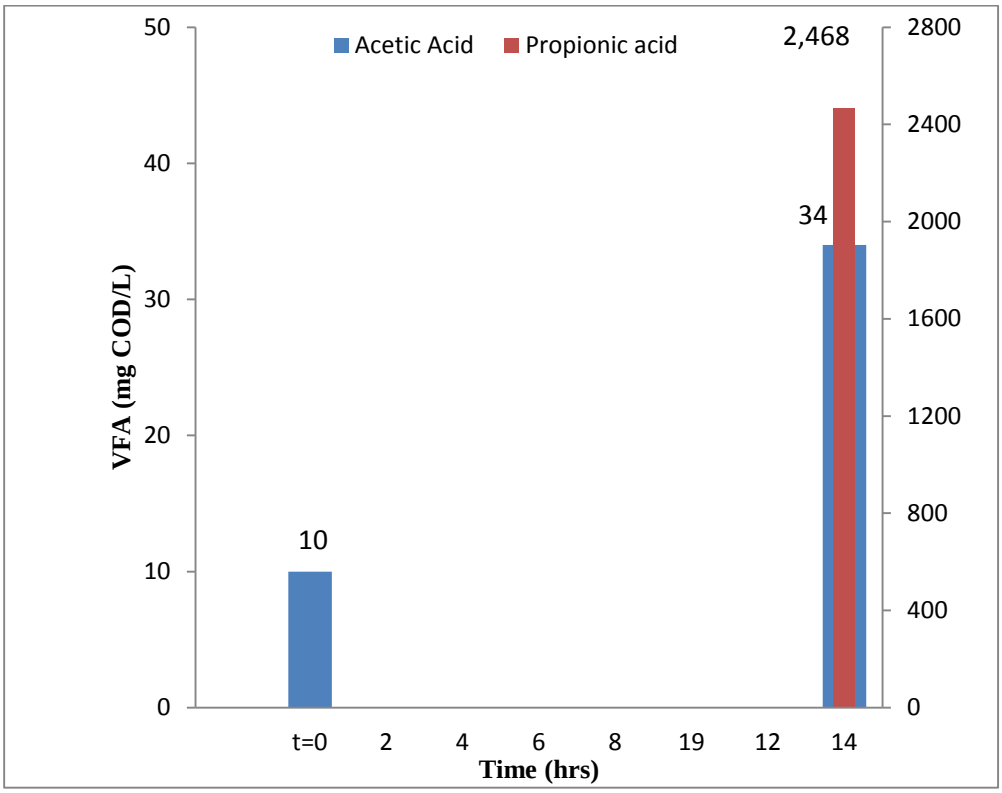

Figure 4.7: Time Series Data for Volatile Fatty Acid (VFA).

Volatile Fatty Acids (VFAs) is one of the key components for the determination of readily biodegradable oxygen demand (RBCOD). RBCOD includes all the VFA and remaining fractions, which are not in the form of VFA but can be converted into VFA. Acetic acid, butyric acid, and

propionic acid are the most common volatile fatty acids in municipal waste. The presence of VFA in influent waste plays the prominent role in the success of Enhance biological phosphorus removal (EBPR).

Glycerol is used as a carbon substrate where bacteria can grow and reproduce. Glycerol is a good carbon source to generate the propionic acid in high quantity with fewer by-products. 50 mg/L glycerol produces 2,468 mg COD/L propionic acid, which represents 98.6 % of total VFAs. The review of other results illustrated glycerol yields as 0.475 propionic g/g glycerol (Liu et al., 2011). In another study of 20 g/L glycerol, the major product formed were propionic acid (0.844 mol/mol), succinic acid (0.055 mol/mol), acetic acid (0.023 mol/mol), and formic acid (0.020 mol/mol) at pH 6.8 (Barbirato et al., 1997). This experiment also suggested the use of glycerol in wastewater by producing abundant VFAs.

4.3 Phase III

In phase three, the first experiment was conducted using 30 mL glycerol stock solution. The second test was conducted using with 30 mL glycerol stock solution, and 5 mL inoculate from glycerol acclimated prefermenter in Nov. 24 and Dec. 2, 2015. The prefermenter was designed to remove significant amount of glycerol. The prefermenter (Figure 4.8) had 1,500 mL primary solids with mixed liquor suspended solid (MLSS) 5,500 mg/L with TSS/VSS ratio as 0.88. Every day, 375 mL was removed and replaced by 6,500 mg glycerol with 375 mL of primary solids and wastewater in 1:1 ratio. The effluent of primary solids contained approximately 8,500 mg/L glycerol. The glycerol content in 5 mL inoculate was approximately 42.5 mg/L, which was about 52 mg COD/L.

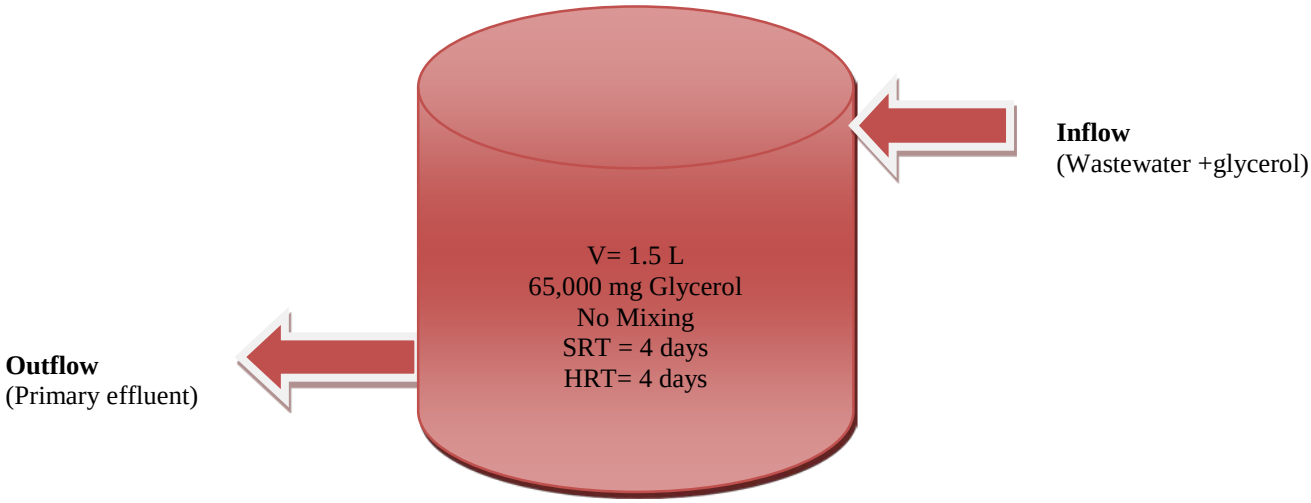

Figure 4.8: Prefermenter.

The addition of 5 mL inoculates containing heterotrophic active mass of 12 mg/L volatile suspended solid (VSS) results in no significant difference in OUR between the two sets of the experiment, as shown in Figure 4.9. One of the reasons might be less primary solids added to the

wastewater. The Z_{BH} of wastewater raised from 5mg COD/L to 10 mg COD/ L (average value 7.5 mg COD/L) when compared with un inoculate and inoculate $Z_{BH.}$

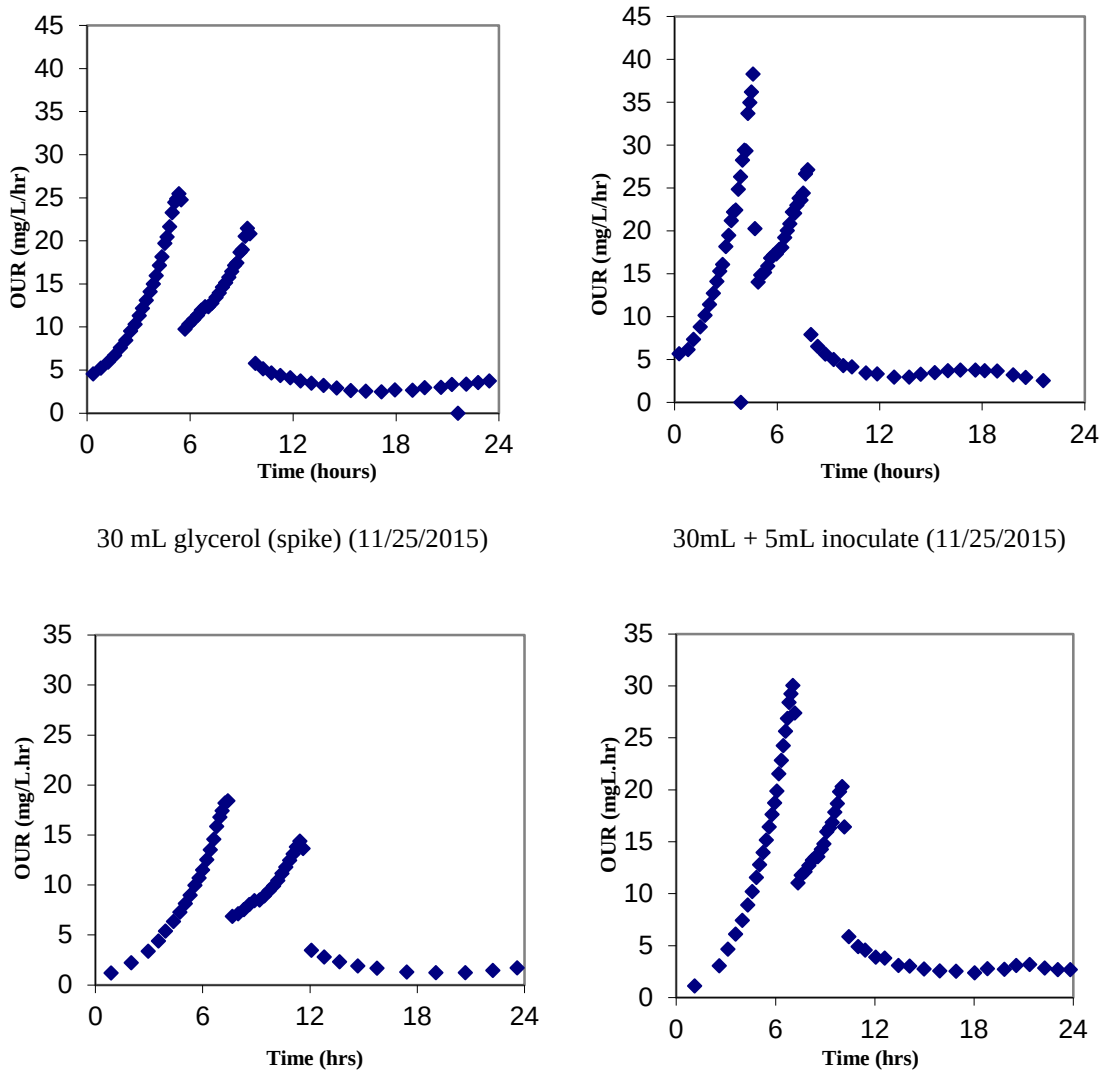

30 mL glycerol (spike) (11/25/2015)

30mL + 5mL inoculate (11/25/2015)

30 mL glycerol (spike) (12/03/2015)

30mL + 5mL inoculate (12/03/2015)

Figure 4.9: Comparison between Spike vs. Spike Plus Inoculate.

The influent wastewater for this batch of the experiment had the highest value of readily oxygen demand than the earlier sample. As the source affects the composition and nature of

wastewater, it might be the possible reason to have high oxygen demand as listed in Table 4-3. The average RBCOD value (2 data points) for 30 mL glycerol spike (control) wastewater was 166 mg COD/L, which is higher than theoretical value (120 mg COD/L). The average RBCOD value for inoculating added wastewater was 190 mg/L, which was also higher than theoretical 172 mg COD/L.

Table 4.3: Results of Phase III Statistical Data

Parameter	Spike		Spike+Inoculate	
	RBCOD(P_1) (mg COD/L)	RBCOD(P_2) (mg COD/L)	RBCOD(P_1) (mg COD/L)	RBCOD(P_2) (mg COD/L)
Minimum Value	100	145	99.0	172
Maximum Value	124	187	152	208
Average Value	112	166	126	190
Standard Deviation	17.0	29.0	37.0	25.0

*Theoretical oxygen demand (TOD) of glycerol is 1.22 mg COD/ mg glycerol and multiply with glycerol dosage 98.5 mg/L (= 120 mg COD/L) and glycerol plus inoculate dosage 141 mg/L (= 172 mg COD/L) to compare data of spike; $P_{1=}$ Peak 1, P_2= Peak 2

4.4 Glycerol Effects

The effect of glycerol on influent wastewater showed the nature of diauxic growth in OUR measurements by delaying the oxygen demand. The subtraction results from the spiked sample with un-spiked sample gave an accurate net effect of glycerol for RBCOD as shown in Figure 4.10. The initial glycerol concentration for the 30 mL and 15 mL glycerol stock solution in wastewater were 120 mg COD/L and 61 mg COD/L, respectively. The average value calculated by the subtraction of oxygen in phase I and phase II were approximately 89 mg COD/L and 55 mg COD/L, respectively, and appeared to be less than the theoretical oxygen demand for glycerol.

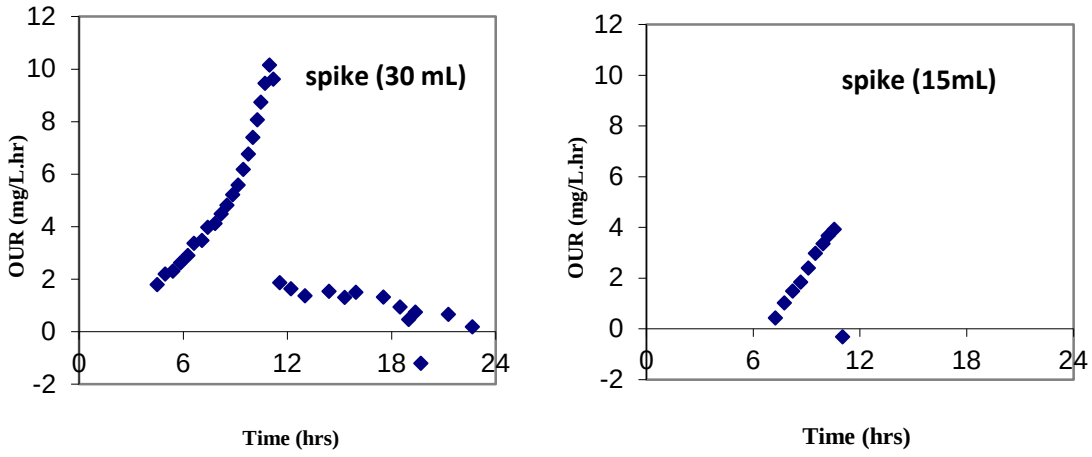

(A= Phase I net glycerol effect)

(B= Phase II net glycerol effect)

Figure 4.10: Glycerol Effect on Phase I and Phase II.

The first phase study showed an increase in the average value of RBCOD from approximately 45 mg COD/L to 89 mg COD/L, which represented about the 97.8 % increment. In the second phase, the average value of RBCOD increased by 17.16 %from 74 mg COD/L to 86.7 mg COD/L. This verified the use of glycerol to produce abundant volatile fatty acids. Another important output was the shift in oxygen demand due to the change in spike volume.

The limited availability of RBCOD hinders a complete removal of nutrients (phosphorus and nitrogen) in wastewater treatment plants (Yuan et al., 2011). The wastewater that has low RBCOD is operated in different COD/P conditions as 25:1, 15:1, and 10:1. In dairy processing wastewater, propionate as a carbon source has high phosphorus removal with COD: P as 13:1 over acetate (Broughton et al., 2007). When sodium acetate is used as a carbon source to determine the RBCOD by single our method, oxygen consumption represents 17 % of COD. When the substrate was increased from the 10 g COD to 18 g COD, the dissolved oxygen increased from the 99.5 to 99.9 % (Ziglio et al., 2001). Methanol is also a carbon source for the increment of the VFAs. However, competition for substrate between the acetogens and methanogens affects the VFA production rate (Taya et al., 2012).

In the influent waste, readily biodegradable substrate is converted into volatile fatty acid by the ordinary heterotrophic organism (OHO) via fermentation process and used by polyphosphate accumulating organisms (PAO) (Wentzel et al., 1985). The presence of VFAs is essential for high removal of phosphorus in wastewater (Randall et al., 1997). The common VFAs found in wastewater are acetic acid and propionic acid. Glycerol is a trihydric alcohol and can be

used as a carbon source to increase the carbon content in wastewater. It can form enormous amount of propionic acid, which contributes to amplify VFA (Barbirato et al., 1997; Yuan et al., 2010). Nowadays, glycerol end product is considered as a suitable substrate for enhanced biological phosphorus removal (Ohemen et al., 2006; Guerrero et al., 2012; Jeon et al., 2000) with nitrification and denitrification (Melidis et al., 2009; Uprety et al., 2013).

4.5 Future Study

This is a limited study for investigating the effect of glycerol on the RBCOD. However, the research highlights the impact of glycerol on chemical oxygen demand as depicted in Figure 4.11 through the oxygen uptake rate (OUR). It mainly focuses on readily biodegradable (RB) substrate and heterotrophic biomass. Slowly biodegradable (SB) substrates are complex compounds and undergo hydrolysis to transform into simpler forms. Heterotrophic biomass utilizes the RB substrate for metabolism and reproduction. Glycerol results in the diauxic growth of bacteria in wastewater. Glycerol accumulating organisms are found active at the lower end of the experimental duration. The value of RBCOD in wastewater increases with the high production of VFAs.

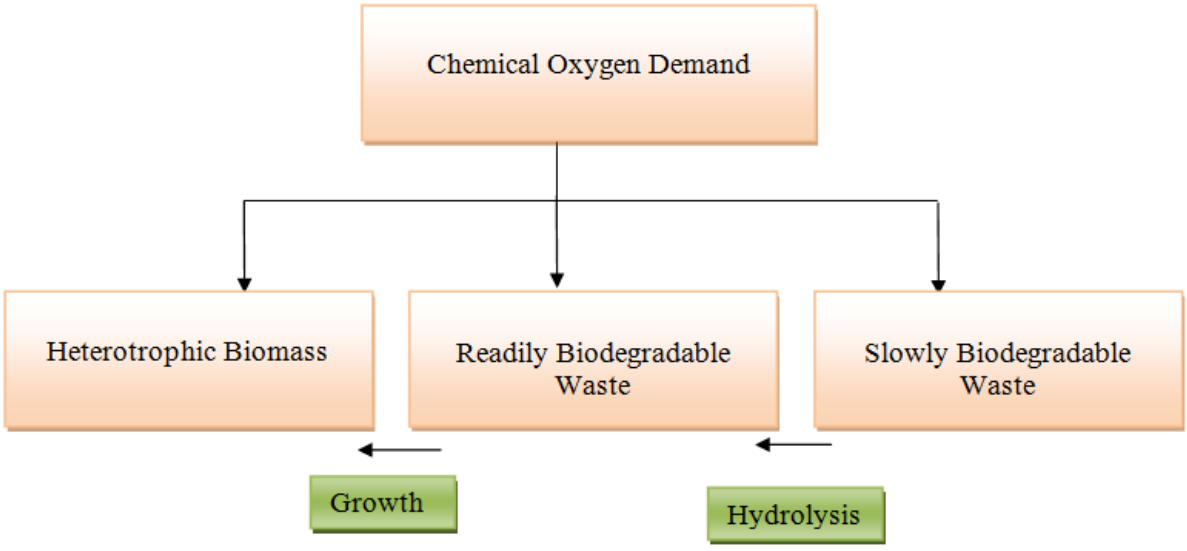

Figure 4.11: Diagram for the Oxygen Demand in Wastewater.

However, due to resource and time constraint, the study is limited to examine the short-term effect of glycerol addition to RBCOD. For future study:

- RBCOD increase from glycerol can be explored to study the effect on effluent nitrogen and phosphorus
- Study other carbon sources like acetic acid, propionic acid, methanol or crude glycerol for RBCOD
- Glycerol can be one of the alternative carbon sources for the low or medium organic content wastewater treatment plant (WWTP).

CHAPTER 5: CONCLUSIONS

The conclusions that can be drawn from the research are:

- Wastewater from Iron Bridge had the low content of RBCOD with 0 mg COD/L to 10 mg COD/L VFA
- Oxygen demand increased by the addition of glycerol due to the diauxic nature of growth
- RBCOD consisted of 12-28 % of TCOD
- Glycerol (50 mg/L) could produce a significant amount of propionic acid (2,502 mg COD/L) which is one of the main components of VFAs.

APPENDIX A:
OXYGEN SOLUBILITY

Table A.1: Oxygen Solubility Table

Temperature (º C)	Dissolved oxygen (mg/L)	Temperature (º C)	Dissolved oxygen (mg/L)
0	14.6	23	8.7
1	14.2	24	8.5
2	13.9	25	8.4
3	13.5	26	8.2
4	13.2	27	8.1
5	12.8	28	7.9
6	12.5	29	7.8
7	12.2	30	7.7
8	11.9	31	7.5
9	11.6	32	7.4
10	11.3	33	7.3
11	11.1	34	7.2
12	10.8	35	7.1
13	10.6	36	7.0
14	10.4	37	6.8
15	10.2	38	6.7
16	9.9	39	6.6
17	9.7	40	6.5
18	9.5	41	6.4
19	9.3	42	6.3
20	9.2	43	6.2
21	9.0	44	6.1
22	8.8	45	6.0

Source: OUR Meter User Guide, University of Cape Town

APPENDIX B:
FORUMULAS

$$\mathbf{RBCOD} = \frac{\mu_H.Z_{BH(0)} .(e^{\text{slope td}}-1)}{Y_{ZH}.\text{slope}.24}$$

Where,

Y_{ZH} = heterotrophic yield, (0.666 mg COD/mg COD)

$\check{u}_H$ = heterotrophic maximum specific growth rate on RBCOD, (d^{-1})

Slope = the slope of ln OUR vs. time (hours)

t_d = time of precipitous drop in OUR, hr

$$\mathbf{Z_{BH}} = \frac{e^{\mathbf{y-intercept}}}{\frac{1-Y_{ZH}\,(\mathbf{slope}.24+\mathbf{bH})}{Y_{ZH}}}$$

Where,

b_H = heterotrophic specific death rate (0.62/day)

Y-intercept = the y-intercept of ln OUR vs. time (in hours)

$$\mathbf{K_{MP}} = \frac{24.\mathbf{OUR}_{\mathbf{SBCOD}\,(\mathbf{ts})}}{\frac{1-Y_{ZH}.Z_{BH}\,e^{(\mathbf{slope\ vs.ts})}}{Y_{ZH}}}$$

Where,

$OUR_{SBCOD\ (ts)}$ = OUR observed immediately the precipitous drop (mg/L.hr)

t_s = time immediately the precipitous drop in OUR (hr)

APPENDIX C:
QUALITY ASSURANCE AND QUALITY CONTROL
(QA & QC)

Table A.2: Quality Assurance (Accuracy)

Date	Un-spike Initial COD (mg COD/L)	Un-spike Final COD (mg COD/L)	% Recovery	Mean	STD. DEV.	UCL	LCL	UWL	LWL
9/1/2015	308	168	71.3	73.2	2.68	81.2	65.2	78.6	67.8
9/2/2015	314	142	75.5	73.2	2.68	81.2	65.2	78.6	67.8
9/24/2015	237	128	74.6	73.2	2.68	81.2	65.2	78.6	67.8
9/25/2016	296	168	70.9	73.2	2.68	81.2	65.2	78.6	67.8
9/28/2015	233	137	78.4	73.2	2.68	81.2	65.2	78.6	67.8
9/29/2015	349	131	71.8	73.2	2.68	81.2	65.2	78.6	67.8
10/1/2015	248	137	72.2	73.2	2.68	81.2	65.2	78.6	67.8
10/14/2015	287	159	71.2	73.2	2.68	81.2	65.2	78.6	67.8

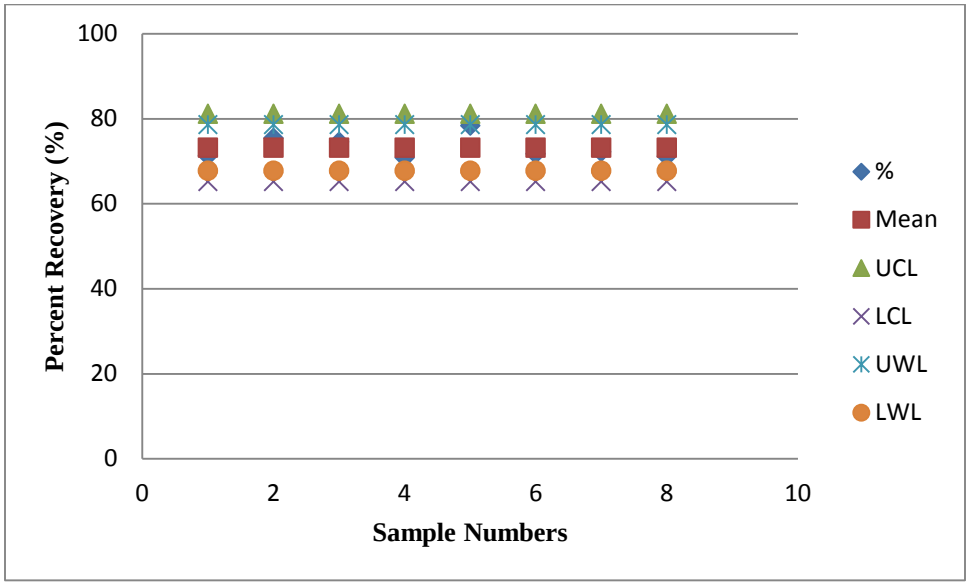

Figure A.1: Accuracy Control Chart for the Study

Table A.3: **Quality Precision for Duplicate Samples**

No of Sample	Initial sample (mg COD/L)	Duplicate Sample (mg COD/L)	Range	I-Statistics	Mean	STD. DEV.	UCL	UWL
1	38.7	37.4	1.30	0.017	0.023	0.005	0.038	0.033
2	32.6	30.9	1.70	0.027	0.023	0.005	0.038	0.033
3	23.5	24.7	1.20	0.025	0.023	0.005	0.038	0.033

APPENDIX D:
UN-SPIKED RAW DATA

Table A.4: Un-spiked Raw Data on 09/01/2015

Cycle number	CTime (mins)	OxOffT (mins)	STime (secs)	ETime (secs)	Slope (mg/L.hr)	CC	SNum	Temp (ºC)
1	137.2	0.7300	6456	9918	1.570	-0.9900	3462	20.40
2	201.0	167.9	1135	2842	3.160	-1.000	1707	21.90
3	239.1	217.2	730.0	1893	4.640	-1.000	1163	22.70
4	267.2	250.8	530.0	1435	5.980	-1.000	905.0	23.30
5	290.1	276.8	424.0	1167	7.260	-1.000	743.0	23.70
6	309.6	298.4	359.0	991.0	8.530	-1.000	632.0	24.00
7	326.9	317.0	310.0	870.0	9.630	-1.000	560.0	24.30
8	433.9	403.8	768.0	2833	2.580	-1.000	2065	25.40
9	484.9	453.4	848.0	2934	2.580	-1.000	2086	25.70
10	530.7	504.8	0.0000	3109	2.570	-0.9900	3109	25.80
11	593.3	559.2	861.0	3223	2.280	-0.9900	2362	25.90
12	792.6	743.8	1101	4760	1.470	-0.9900	3659	26.50
13	881.4	826.3	1165	5450	1.250	-0.9700	4285	26.60
14	980.8	921.4	1212	5921	1.120	-0.9500	4709	26.60
15	1078	1025	1102	5314	1.280	-0.9700	4212	26.70
16	1174	1123	1015	5126	1.300	-0.9800	4111	26.90
17	1263	1212	1099	4974	1.380	-0.9800	3875	27.10

*Note: CTime= Current Time, OxoffT= Air off Time, STime= Start Time, CC= correlation coefficient, SNum= No. of Samples, Temp= Temperature (ºC)

Table A.5: Un-spiked Raw Data on 09/02/2015

Cycle number	CTime (mins)	OxOffT (mins)	STime (secs)	ETime (secs)	Slope (mg/L.hr)	CC	SNum	Temp (°C)
1	83.67	0.0000	3829	6211	2.260	-1.000	2382	22.10
2	165.0	145.7	576.0	1739	4.680	-1.000	1163	23.00
3	191.7	176.2	465.0	1404	5.770	-1.000	939.0	24.30
4	213.8	201.0	378.0	1155	6.890	-1.000	777.0	23.80
5	249.8	239.9	282.0	902.0	8.840	-1.000	620.0	24.10
6	424.6	376.1	1234	4586	1.610	-0.9900	3352	24.60
7	507.1	453.8	1307	5082	1.420	-0.9900	3775	24.80
8	596.8	539.8	1403	5436	1.330	-0.9800	4033	25.00
9	702.9	631.7	1530	7018	0.9600	-0.8700	5488	25.10
10	514.0	749.9	2191	-30500	0.0700	-0.0400	30576	26.30

*Note: CTime= Current Time, OxoffT= Air off Time, STime= Start Time, CC= correlation coefficient, SNum= No. of Samples, Temp= Temperature (°C)

Table A.6: Un-spiked Raw Data on 09/24/2015

Cycle number	CTime (mins)	OxOffT (mins)	STime (secs)	ETime (secs)	Slope (mg/L.hr)	CC	SNum	Temp (°C)
1	22.40	4.180	515.0	1672	4.650	-1.000	1157	24.50
2	50.28	34.55	456.0	1432	5.520	-1.000	976.0	24.70
3	74.72	61.05	401.0	1239	6.430	-1.000	838.0	24.90
4	96.59	84.37	360.0	1106	7.230	-1.000	746.0	25.20
5	116.4	105.5	322.0	984.0	8.150	-1.000	662.0	25.40
6	134.4	124.7	286.0	877.0	9.150	-1.000	591.0	25.60
7	150.8	142.1	259.0	792.0	10.14	-1.000	533.0	25.70
8	166.0	158.0	237.0	723.0	11.11	-1.000	486.0	25.80
9	180.4	172.9	222.0	679.0	11.84	-1.000	457.0	25.90
10	196.1	186.9	213.0	889.0	8.010	-0.990	676.0	26.00
11	223.9	204.2	517.0	1852	3.990	-1.000	1335	26.30
12	343.3	316.9	702.0	2457	3.090	-1.000	1755	26.80
13	438.6	406.6	822.0	3009	2.450	-0.9900	2187	27.00
14	488.6	458.7	1.000	3585	2.260	-0.9700	3584	27.00
15	565.4	520.4	1078	4323	1.660	-0.9900	3245	26.90
16	639.6	594.4	1289	4146	1.450	-0.9900	2857	26.80
17	871.5	778.6	1732	9424	0.6800	-0.5900	7692	26.60
18	1057	937.4	2081	12211	0.4500	-0.4000	10130	26.20

*Note: CTime= Current Time, OxoffT= Air off Time, STime= Start Time, CC= correlation coefficient, SNum= No. of Samples, Temp= Temperature (°C)

Table A.7: Un-spiked Raw Data on 09/25/2015

Cycle number	CTime (mins)	OxOffT (mins)	STime (secs)	ETime (secs)	Slope (mg/L.hr)	CC	SNum	Temp (ºC)
1	51.13	2.250	1787	4078	2.330	-1.000	2291	18.10
2	102.8	72.05	1103	2589	3.610	-1.000	1486	19.50
3	170.8	152.0	634.0	1623	5.490	-1.000	989.0	21.20
4	196.8	180.9	538.0	1365	6.480	-1.000	827.p	21.70
5	240.8	227.9	425.0	1115	7.820	-1.000	690.0	22.40
6	333.9	299.2	1096	3075	2.690	-1.000	1979	23.50
7	389.6	352.3	1147	3335	2.500	-1.000	2188	23.90
8	447.0	409.6	1121	3366	2.400	-1.000	2245	24.10
9	508.3	467.5	1230	3671	2.250	-1.000	2441	24.40
10	576.0	530.4	1359	4122	1.940	-0.9900	2763	24.60
11	653.9	600.7	1503	4876	1.580	-0.9900	3373	24.70
12	748.4	683.6	1765	6013	1.260	-0.9700	4248	24.80
13	864.5	785.5	2015	7476	0.9800	-0.8700	5461	24.60
14	1015	911.7	2408	10048	0.6800	-0.6100	7640	24.40
15	1209	1081	2941	12403	0.5600	-0.4200	9462	24.90

Note: CTime= Current Time, OxoffT= Air off Time, STime= Start Time, CC= correlation coefficient, SNum= No. of Samples, Temp= Temperature (ºC)

Table A.8: Un-spiked Raw Data on 09/28/2015

Cycle number	CTime (mins)	OxOffT (mins)	STime (secs)	ETime (secs)	Slope (mg/L.hr)	CC	SNum	Temp (°C)
1	114.4	2.970	4934	8440	1.540	-0.9900	3506	18.80
2	215.2	193.9	710.0	1845	4.760	-1.000	1135	21.40
3	243.3	227.1	536.0	1420	6.110	-1.000	884.0	22.10
4	266.4	253.1	437.0	1172	7.340	-1.000	735.0	22.60
5	286.6	275.0	376.0	1016	8.410	-1.000	640.0	23.00
6	304.5	294.4	328.0	885.0	9.660	-1.000	557.0	23.30
7	349.1	327.4	291.0	2318	2.430	-0.9900	2027	24.20
8	400.9	368.2	963.0	2969	2.690	-1.000	2006	24.90
9	452.9	419.8	918.0	3051	2.530	-1.000	2133	25.30
10	505.4	472.7	915.0	3001	2.580	-1.000	2086	25.70
11	557.9	524.8	916.0	3060	2.510	-1.000	2144	25.90
12	757.0	704.2	1287	5055	1.410	-0.9800	3768	26.70
13	855.1	790.3	1511	6263	1.120	-0.9400	4752	27.10
14	957.9	896.6	0.0000	7371	1.120	-0.4500	7371	27.30

Note: CTime= Current Time, OxoffT= Air off Time, STime= Start Time, CC= correlation coefficient, SNum= No. of Samples, Temp= Temperature (°C)

Table A.9: Un-spiked Raw Data on 09/29/2015

Cycle number	CTime (mins)	OxOffT (mins)	STime (secs)	ETime (secs)	Slope (mg/L.hr)	CC	SNum	Temp (ºC)
1	104.9	85.53	668.0	1666	5.430	-1.000	998.0	20.70
2	132.2	115.8	565.0	1403	6.450	-1.000	838.0	21.30
3	155.7	141.7	454.0	1219	7.170	-1.000	765.0	21.70
4	177.0	164.6	418.0	1070	8.320	-1.000	652.0	22.10
5	196.5	185.1	381.0	985.0	8.910	-1.000	604.0	22.40
6	214.6	204.2	349.0	899.0	9.820	-1.000	550.0	22.70
7	236.9	221.8	326.0	1486	4.150	-0.9700	1160	23.00
8	280.5	248.8	1018	2785	3.050	-1.000	1767	23.50
9	328.6	297.6	980.0	2748	3.030	-1.000	1768	23.90
10	378.3	345.62	1017	2898	2.840	-1.000	1881	24.20
11	429.9	396.1	1033	3020	2.750	-1.000	1987	24.40
12	484.2	448.6	1123	3148	2.650	-1.000	2025	24.50
13	596.9	559.5	1157	3333	2.490	-1.000	2176	24.90
14	658.1	617.0	1253	3673	2.240	-0.9900	2420	25.00
15	726.0	680.2	1357	4142	1.950	-0.9900	2785	25.10
16	803.7	751.2	1535	4761	1.670	-0.9900	3226	25.10
17	888.7	832.5	1686	5054	1.610	-0.9900	3368	25.20
18	973.8	918.6	1661	4957	1.630	-0.9900	3296	25.50
19	1057	1003	1628	4806	1.690	-0.9900	3178	25.70
20	1139	1085	1599	4881	1.650	-0.9900	3282	25.80
21	1226	1168	1636	5217	1.50	-0.9900	3581	26.00
22	1320	1257	1805	5745	1.370	-0.9800	3940	26.20

Note: CTime= Current Time, OxoffT= Air off Time, STime= Start Time, CC= correlation coefficient, SNum= No. of Samples, Temp= Temperature (ºC)

Table A.10: Un-spiked Raw Data on 10/01/2015

Cycle number	CTime (mins)	OxOffT (mins)	STime (secs)	ETime (secs)	Slope (mg/L.hr)	CC	SNum	Temp (ºC)
1	66.98	3.500	2190	5428	1.660	-0.9900	3238	18.50
2	122.4	97.33	148.0	2855	2.910	-0.9900	2707	20.60
3	171.4	148.7	687.0	2028	4.050	-1.000	1341	21.80
4	230.9	217.0	389.0	1277	6.130	-1.000	888.0	23.40
5	255.4	243.5	337.0	1095	7.140	-1.000	758.0	24.00
6	279.5	268.9	315.0	955.0	8.490	-1.000	640.0	24.50
7	299.9	291.3	224.0	811.0	9.260	-1.000	587.0	24.90
8	322.8	314.9	204.0	735.0	10.19	-1.000	531.0	25.30
9	353.6	338.7	299.0	1495	4.480	-1.000	1196	25.90
10	388.7	371.9	407.0	1600	4.530	-1.000	1193	26.40
11	431.7	415.2	358.0	1627	4.260	-1.000	1269	26.90

Note: CTime= Current Time, OxoffT= Air off Time, STime= Start Time, CC= correlation coefficient, SNum= No. of Samples, Temp= Temperature (ºC)

Table A.11: Un-spiked Raw Data on 10/14/2015

Cycle number	CTime (mins)	OxOffT (mins)	STime (secs)	ETime (secs)	Slope (mg/L.hr)	CC	SNum	Temp (ºC)
1	25.72	4.130	0.0000	2591	2.790	-0.9700	2591	21.70
2	73.22	51.45	628.0	1984	4.000	-1.000	1356	22.50
3	230.9	223.55	212.0	680.0	11.59	-1.000	468.0	24.70
4	246.0	239.18	193.0	625.0	12.48	-1.000	432.0	24.80
5	273.6	267.88	165.0	522.0	15.08	-1.000	357.0	25.00
6	315.1	305.92	151.0	954.0	5.900	-0.9800	803.0	25.30
7	372.4	355.02	487.0	1598	4.870	-1.000	1111	25.70
8	403.0	384.58	492.0	1719	4.400	-1.000	1227	25.80
9	435.7	416.07	535.0	1815	4.230	-1.000	1280	25.90
10	469.4	449.07	559.0	1882	4.100	-1.000	1323	26.00
11	598.4	564.17	855.0	3256	2.240	-0.9900	2401	25.90
12	667.7	620.93	1089	4518	1.550	-0.9900	3429	25.90
13	1035	818.22	1955	24007	0.1700	-0.0800	22052	25.30
14	1312	1220.7	2063	8886	0.7800	-0.7100	6823	25.50

Note: CTime= Current Time, OxoffT= Air off Time, STime= Start Time, CC= correlation coefficient, SNum= No. of Samples, Temp= Temperature (ºC)

APPENDIX E:
SPIKED SAMPLE DATA (30 mL)

Table A.12: Spiked Raw Data on 09/01/2015

Cycle number	CTime (mins)	OxOffT (mins)	STime (secs)	ETime (secs)	Slope (mg/L.hr)	CC	SNum	Temp (°C)
1	45.85	7.930	1084	3467	2.260	-1.000	2383	19.90
2	134.7	119.3	444.0	1413	5.570	-1.000	969.0	22.50
3	159.0	145.8	393.0	1186	6.800	-1.000	793.0	23.10
4	179.7	168.2	352.0	1025	7.990	-1.000	673.0	23.60
5	246.9	224.8	681.0	1971	4.180	-1.000	1290	25.00
6	278.8	259.5	592.0	1724	4.780	-1.000	1132	25.40
7	334.0	316.6	513.0	1584	5.030	-1.000	1071	26.00
8	413.0	398.5	409.0	1336	5.830	-1.000	927.0	26.70
9	436.9	423.2	393.0	1261	6.200	-1.000	868.0	26.90
10	521.8	510.6	315.0	1025	7.590	-1.000	710.0	27.40
11	540.9	530.3	298.0	982.0	7.920	-1.000	684.0	27.50
12	577.7	567.6	289.0	923.0	8.470	-1.000	634.0	27.60
13	612.5	602.6	298.0	897.0	9.040	-1.000	599.0	27.70
14	629.2	619.6	290.0	865.0	9.400	-1.000	575.0	27.80
15	645.4	635.9	289.0	846.0	9.750	-1.000	557.0	27.80
16	676.2	667.3	283.0	790.0	10.63	-1.000	507.0	27.80
17	690.9	682.2	277.0	769.0	11.01	-1.000	492.0	27.90
18	705.2	696.7	273.0	756.0	11.23	-1.000	483.0	27.90
19	719.6	710.9	276.0	765.0	11.06	-1.000	489.0	27.90
20	789.9	760.1	880.0	2690	2.970	-1.000	1810	27.80
21	837.8	806.4	933.0	2837	2.830	-1.000	1904	27.60
22	887.6	855.1	977.0	2927	2.760	-1.000	1950	27.50
23	938.5	905.2	994.0	2992	2.670	-1.000	1998	27.40
24	989.2	956.4	1006	2922	2.810	-1.000	1916	27.40
25	1139	1106	1019	2974	2.760	-1.000	1955	27.70
26	1246	1209	1081	3269	2.470	-0.9900	2188	27.80
27	1371	1326	1262	4108	1.890	-0.9900	2846	28.00

Note: CTime= Current Time, OxoffT= Air off Time, STime= Start Time, CC= correlation coefficient, SNum= No. of Samples, Temp= Temperature (°C)

Table A.13: Spiked Raw Data on 09/02/2015

Cycle number	CTime (mins)	OxOffT (mins)	STime (secs)	ETime (secs)	Slope (mg/L.hr)	CC	SNum	Temp (ºC)
1	33.83	2.000	0.0000	3819	2.280	-0.9400	3819	20.70
2	94.26	67.28	859.0	2378	3.570	-1.000	1519	21.70
3	128.8	108.7	633.0	1781	4.760	-1.000	1148	22.40
4	151.9	140.1	1.000	1425	5.840	-1.000	1424	22.90
5	198.8	187.3	360.0	1028	8.020	-1.000	668.0	23.50
6	332.7	314.7	1.000	2155	3.820	-1.000	2154	25.00
7	407.9	386.7	634.0	1913	4.160	-1.000	1279	25.50
8	471.3	452.2	538.0	1750	4.510	-1.000	1212	25.80
9	586.6	5698	501.0	1524	5.300	-1.000	1023	26.10
10	637.4	622.4	445.0	1360	5.900	-1.000	915.0	26.20
11	660.7	646.6	411.0	1291	6.170	-1.000	880.0	26.30
12	761.9	750.7	341.0	997.0	8.220	-1.000	656.0	26.20
13	795.6	786.0	276.0	867.0	9.150	-1.000	591.0	26.10
14	826.3	817.6	252.0	799.0	9.850	-1.000	547.0	26.10
15	877.5	848.5	677.0	2807	2.570	-1.000	2130	25.90
16	929.7	896.7	953.0	3001	2.590	-1.000	2048	25.80
17	979.3	948.3	879.0	2846	2.720	-1.000	1967	25.90
18	1027	997.2	842.0	2759	2.810	-1.000	1917	25.90
19	1175	1141	918.0	3098	2.460	-1.000	2180	26.10
20	1299	1255	1097	4143	1.760	-0.9900	3046	26.30
21	1380	1326	1309	5281	1.350	-0.9800	3972	26.40

Note: CTime= Current Time, OxoffT= Air off Time, STime= Start Time, CC= correlation coefficient, SNum= No. of Samples, Temp= Temperature (ºC)

Table A.14: Spiked Raw Data on 09/24/2015

Cycle number	CTime (mins)	OxOffT (mins)	STime (secs)	ETime (secs)	Slope (mg/L.hr)	CC	SNum	Temp (ºC)
1	28.74	3.130	792.0	2281	3.590	-1.000	1489	24.70
2	89.94	73.82	503.0	1432	5.730	-1.000	929.0	25.10
3	113.2	99.33	436.0	1233	6.890	-1.000	797.0	25.20
4	133.6	121.5	390.0	1067	7.970	-1.000	677.0	25.30
5	151.6	140.9	344.0	936.0	9.060	-1.000	592.0	25.40
6	196.1	188.1	251.0	705.0	12.07	-1.000	454.0	25.50
7	264.9	237.6	858.0	2412	3.470	-1.000	1554	25.70
8	306.9	279.3	834.0	2490	3.240	-1.000	1656	25.90
9	349.9	322.2	872.0	2454	3.440	-1.000	1582	26.00
10	390.5	364.5	831.0	2298	3.680	-1.000	1467	26.00
11	429.1	404.1	806.0	2187	3.920	-1.000	1381	26.00
12	465.7	441.9	782.0	2067	4.230	-1.000	1285	26.10
13	499.1	477.7	714.0	1850	4.760	-1.000	1136	26.10
14	529.0	509.9	640.0	1654	5.300	-1.000	1014	26.00
15	580.5	565.1	519.0	1328	6.710	-1.000	809.0	25.90
16	602.6	588.6	484.0	1199	7.580	-1.000	715.0	25.90
17	622.3	609.9	425.0	1063	8.460	-1.000	638.0	25.90
18	640.1	628.9	383.0	962.0	9.420	-1.000	579.0	25.80
19	671.3	662.1	317.0	782.0	11.65	-1.000	465.0	25.80
20	684.9	676.6	292.0	709.	12.87	-1.000	417.0.	25.80
21	708.7	701.9	238.0	586.0	15.57	-1.000	348.0	25.80
22	719.5	713.0	225.0	546.0	16.64	-1.000	321.0	25.80
23	741.3	723.5	211.0	1921	2.150	-0.9200	1710	25.70
24	825.8	756.8	1818	6470	1.140	-0.9500	4652	25.60
25	939.2	865.9	2058	6742	1.040	-0.9600	4684	25.50
26	994.5	979.6	66.00	1725	2.160	-0.9300	1659	25.50
27	1025	1009	65.00	1906	2.200	-0.9700	1841	25.30
28	1056	1041	63.00	1697	2.180	-0.9500	1634	25.20
29	1084	1071	59.00	1547	2.340	-0.9100	1488	25.10
30	1111	1097	66.00	1557	2.380	-0.9500	1491	25.00
31	1142	1124	71.00	2145	1.890	-0.9600	2074	24.80
32	1181	1160	43.00	2421	1.680	-0.9500	2378	24.70
33	1225	1201	65.00	2771	1.620	-0.9800	2706	24.60
34	1266	1249	50.00	2019	1.990	-0.9800	1969	24.50
35	1357	1283	63.00	8854	0.540	-0.2900	8791	24.60

Note: CTime= Current Time, OxoffT= Air off Time, STime= Start Time, CC= correlation coefficient, SNum= No. of Samples, Temp= Temperature (ºC)

Table A.15: Spiked Raw Data on 09/25/2015

Cycle number	CTime (mins)	OxOffT (mins)	STime (secs)	ETime (secs)	Slope (mg/L.hr)	CC	SNum	Temp (ºC)
1	65.45	0.0000	2845	5009	2.500	-1.000	2164	18.40
2	142.8	123.85	619.0	1658	5.190	-1.000	1039	21.20
3	169.0	153.4	498.0	1375	6.150	-1.000	877.0	22.00
4	191.6	178.25	426.0	1181	7.180	-1.000	755.0	22.60
5	211.6	199.9	370.0	1037	8.130	-1.000	667.0	23.20
6	229.9	219.1	338.0	956	8.760	-1.000	618.0	23.60
7	255.6	237.1	391.0	1838	3.660	-1.000	1447	24.20
8	291.8	269.5	676.0	1994	4.100	-1.000	1318	24.70
9	326.5	304.6	645.0	1982	4.050	-1.000	1337	25.20
10	360.9	339.5	640.0	1923	4.190	-1.000	1283	25.50
11	393.9	373.3	610.0	1864	4.300	-1.000	1254	25.80
12	426.6	406.2	600.0	1849	4.330	-1.000	1249	26.00
13	491.8	471.4	607.0	1846	4.370	-1.000	1239	26.30
14	524.1	503.8	604.0	1824	4.400	-1.000	1220	26.50
15	587.1	567.5	590.0	1759	4.610	-1.000	1169	26.70
16	646.7	628.6	559.0	1611	5.100	-1.000	1052	26.90
17	674.2	657.3	524.0	1503	5.490	-1.000	979.0	27.00
18	699.6	684.0	487.0	1389	5.970	-1.000	902.0	27.00
19	723.4	708.9	459.0	1282	6.540	-1.000	823.0	27.00
20	745.2	731.9	419.0	1168	7.190	-1.000	749.0	27.00
21	783.6	772.6	352.0	970.0	8.720	-1.000	618.0	27.00
22	800.6	790.6	319.0	887.0	9.560	-1.000	568.0	27.00
23	816.6	807.2	302.0	834.0	10.21	-1.000	532.0	27.00
24	832.2	822.8	291.0	835.0	10.00	-1.000	544.0	27.00
25	1005	958.5	1251	4339	1.740	-0.9900	3088	26.60
26	1154	1107.	1242	4307	1.760	-0.9900	3065	26.80
27	1227	1181	1245	4312	1.750	-0.9900	3067	27.00
28	1302	12545	1257	4404	1.700	-0.9900	3147	27.30
29	1379	1330	1279	4651	1.590	-0.9900	3372	27.50

Note: CTime= Current Time, OxoffT= Air off Time, STime= Start Time, CC= correlation coefficient, SNum= No. of Samples, Temp= Temperature (ºC)

Table A.16: Spiked Raw Data on 09/28/2015

Cycle number	CTime (mins)	OxOffT (mins)	STime (secs)	ETime (secs)	Slope (mg/L.hr)	CC	SNum	Temp (ºC)
1	102.0	3.080	4140	7734	1.500	-0.9900	3594	18.50
2	174.5	134.1	1485	3362	2.890	-1.000	1877	20.00
3	219.1	192.4	933.0	2279	4.030	-1.000	1346	20.90
4	253.0	232.6	696.0	1755	5.080	-1.000	1059	21.40
5	281.3	264.2	580.0	1475	5.950	-1.000	895.0	21.80
6	305.8	291.1	490.0	1275	6.850	-1.000	785.0	22.10
7	327.1	314.7	403.0	1089	7.810	-1.000	686.0	22.40
8	346.2	335.3	354.0	959.0	8.900	-1.000	605.0	22.60
9	363.6	353.7	317.0	869.0	9.670	-1.000	552.0	22.70
10	452.8	419.34	1084	2934	2.930	-1.000	1850	23.50
11	500.1	470.4	930.0	2640	3.140	-1.000	1710	23.70
12	543.5	516.4	871.0	2380	3.560	-1.000	1509	23.90
13	582.5	558.1	770.0	2160	3.920	-1.000	1390	24.00
14	618.3	596.1	699.0	1961	4.340	-1.000	1262	24.00
15	651.2	630.7	663.0	1784	4.840	-1.000	1121	24.10
16	680.5	662.4	599.0	1572	5.510	-1.000	973.0	24.20
17	706.9	690.6	540.0	1413	6.140	-1.000	873.0	24.30
18	730.8	716.2	485.0	1278	6.900	-1.000	793.0	24.40
19	771.7	760.2	381.0	1010	8.540	-1.000	629.0	24.50
20	789.2	778.9	331.0	898.0	9.430	-1.000	567.0	24.60
21	805.1	795.9	289.0	811.0	10.44	-1.000	522.0	24.70
22	819.9	811.5	266.0	745.0	11.35	-1.000	479.0	24.70
23	833.8	826.0	241.0	691.0	12.37	-1.000	450.0	24.80
24	855.9	839.6	240.0	1717	2.770	-0.9300	1477	24.80
25	924.6	870.1	1500	5046	1.510	-0.9900	3546	25.00
26	1020	956.1	1787	5888	1.320	-0.9800	4101	25.00
27	1125	1056	1916	6322	1.200	-0.9600	4406	24.80
28	12374	1163	2056	6797	1.150	-0.9400	4741	24.50
29	1352	1278	2104	6745	1.170	-0.9500	4641	24.50

Note: CTime= Current Time, OxoffT= Air off Time, STime= Start Time, CC= correlation coefficient, SNum= No. of Samples, Temp= Temperature (ºC)

Table A.17: Spiked Raw Data on 10/29/2015

Cycle number	CTime (mins)	OxOffT (mins)	STime (secs)	ETime (secs)	Slope (mg/L.hr)	CC	SNum	Temp (ºC)
1	29.98	2.080	884.0	2464	3.420	-1.000	1580	18.40
2	66.95	45.22	714.0	1894	4.570	-1.000	1180	19.70
3	95.79	78.90	551.0	1476	5.830	-1.000	925.0	20.60
4	139.6	127.9	376.0	1023	8.340	-1.000	647.0	21.90
5	157.3	147.2	321.0	893.0	9.470	-1.000	572.0	22.40
6	173.3	164.3	287.0	793.0	10.63	-1.000	506.0	22.80
7	201.6	194.0	239.0	665.0	12.68	-1.000	426.0	23.40
8	215.2	207.4	231.0	710.0	11.70	-1.000	479.0	23.70
9	240.2	221.2	571.0	1713	4.710	-1.000	1142	24.30
10	269.4	251.7	532.0	1590	5.120	-1.000	1058	24.70
11	296.9	280.2	498.0	1519	5.240	-1.000	1021	25.10
12	324.2	307.4	505.0	1510	5.340	-1.000	1005	25.30
13	350.5	334.5	479.0	1445	5.570	-1.000	966	25.60
14	376.0	360.5	463.0	1401	5.750	-1.000	938	25.70
15	424.5	410.0	433.0	1302	6.230	-1.000	869.0	26.00
16	469.7	456.3	407.0	1203	6.800	-1.000	796.0	26.10
17	491.0	478.2	395.0	1151	7.150	-1.000	756.0	26.20
18	511.4	499.1	378.0	1099	7.490	-1.000	721.0	26.30
19	531.1	519.2	371.0	1052	7.920	-1.000	681.0	26.40
20	549.7	538.5	343.0	1000	8.220	-1.000	657.0	26.40
21	567.7	556.9	331.0	954.0	8.760	-1.000	623.0	26.50
22	584.7	574.6	312.0	894.0	9.300	-1.000	582.0	26.60
23	600.8	591.3	297.0	845.0	9.870	-1.000	548.0	26.70
24	616.1	607.2	278.0	796.0	10.48	-1.000	518.0	26.70
25	657.8	650.2	240.0	676.0	12.40	-1.000	436.0	26.80
26	671.1	663.3	234.0	699.0	11.80	-1.000	465.0	26.90
27	781.1	754.0	771.0	2486	3.120	-1.000	1715	27.00
28	825.5	797.1	806.0	2598	3.000	-1.000	1792	27.00
29	917.6	888.1	848.0	2685	2.920	-1.000	1837	27.10
30	1109	1077	889.0	2950	2.600	-0.9900	2061	27.60
31	1162	1128	915.0	3174	2.360	-0.9900	2259	27.70
32	1220	1183	969.0	3526	2.120	-0.9900	2557	27.80
33	1359	1311	1162	4540	1.590	-0.9900	3378	28.10

Note: CTime= Current Time, OxoffT= Air off Time, STime= Start Time, CC= correlation coefficient, SNum= No. of Samples, Temp= Temperature (ºC)

Table A.18: Spiked Raw Data on 12/03/2015

Cycle number	CTime (mins)	OxOffT (mins)	STime (secs)	ETime (secs)	Slope (mg/L.hr)	CC	SNum	Temp (ºC)
1	52.54	2.900	832.0	5125	1.200	-0.9700	4293	17.30
2	176. 8	151.4	726.0	2323	3.390	-1.000	1597	20.60
3	211.2	192.0	542.0	1763	4.420	-1.000	1221	21.30
4	262.2	248.9	366.0	1217	6.350	-1.000	851.0	22.30
5	282.8	271.2	325.0	1063	7.280	-1.000	738.0	22.60
6	301.0	290.8	276.0	942.0	8.150	-1.000	666.0	22.90
7	317.8	308.6	255.0	857.0	8.990	-1.000	602.0	23.20
8	333.3	324.8	238.0	779.0	9.980	-1.000	541.0	23.30
9	347.6	339.8	215.	727.0	10.71	-1.000	512.0	23.50
10	373.7	367.0	184.0	611.0	12.55	-1.000	427.0	23.80
11	385.3	379.2	166.0	566.0	13.54	-1.000	400.0	23.90
12	396.6	390.7	171.0	536.0	14.58	-1.000	365.0	24.00
13	407.0	401.7	150.0	496.0	15.87	-1.000	346.0	24.10
14	417.0	412.0	140.0	460.0	16.78	-1.000	320.0	24.20
15	444.8	440.4	122.0	417.0	18.44	-1.000	295.0	24.40
16	459.3	449.3	202.0	1000	6.870	-1.000	798.0	24.50
17	479.0	467.6	306.0	1068	7.120	-1.000	762.0	24.60
18	498.1	487.1	303.0	1026	7.530	-1.000	723.0	24.70
19	516.3	505.9	298.0	960.0	8.040	-1.000	662.0	24.80
20	533.6	523.5	281.0	926.0	8.430	-1.000	645.0	24.80
21	550.5	540.6	273.0	912.0	8.490	-1.000	639.0	24.90
22	566.9	557.4	274.0	873.0	8.930	-1.000	599.0	24.90
23	582.5	573.5	251.0	827.0	9.440	-1.000	576.0	25.00
24	597.6	588.9	249.0	794.0	9.920	-1.000	545.0	25.00
25	611.9	603.8	235.0	751.0	10.47	-1.000	516.0	25.00
26	625.7	617.8	230.0	719.0	11.16	-1.000	489.0	25.00
27	638.7	631.4	210.0	670.0	11.80	-1.000	460.0	25.00
28	651.4	644.2	219.0	651.0	12.47	-1.000	432.0	25.00
29	663.3	656.6	197.0	609.0	13.12	-1.000	412.0	25.10
30	674.7	668.3	187.0	580.0	13.81	-1.000	393.0	25.10
31	685.7	679.6	181.0	554.0	14.38	-1.000	373.0	25.10
32	696.7	690.4	180.0	584.0	13.64	-1.000	404.0	25.10
33	724.6	701.5	599.0	2157	3.470	-1.000	1558	25.10
34	767.5	738.9	763.0	2677	2.800	-1.000	1914	25.10
35	818.9	784.8	898.0	3193	2.320	-0.9900	2295	25.10
36	880.2	839.4	1045	3849	1.920	-0.9900	2804	25.00
37	1044.7	985.7	1477	5599	1.290	-0.9800	4122	24.80
38	1142.7	1080	1595	5876	1.240	-0.9700	4281	24.60
39	1241.1	1178	1590	5783	1.250	-0.9800	4193	24.40
40	1333.6	1277	1539	5199	1.470	-0.9900	3660	24.40

Note: CTime= Current Time, OxoffT= Air off Time, STime= Start Time, CC= correlation coefficient, SNum= No. of Samples, Temp= Temperature (ºC)

Table A.19: Spiked Raw Data on 11/25/2015

Cycle number	CTime (mins)	OxOffT (mins)	STime (secs)	ETime (secs)	Slope (mg/L.hr)	CC	SNum	Temp (ºC)
1	20.96	3.700	439.0	1632	4.550	-1.000	1193	22.60
2	47.99	33.15	375.0	1406	5.220	-1.000	1031	22.80
3	73.25	58.93	401.0	1317	5.940	-1.000	916.0	22.90
4	95.72	83.23	345.0	1154	6.700	-1.000	809.0	23.10
5	116.2	104.8	331.0	1039	7.590	-1.000	708.0	23.30
6	134.6	124.4	299.0	935.0	8.440	-1.000	636.0	23.50
7	152.1	142.4	299.0	868.0	9.530	-1.000	569.0	23.60
8	167.6	159.2	244.0	765.0	10.33	-1.000	521.0	23.70
9	182.1	174.3	233.0	709.0	11.32	-1.000	476.0	23.80
10	220.3	214.0	185.0	569.0	14.10	-1.000	384.0	24.10
11	231.8	225.8	174.0	535.0	14.99	-1.000	361.0	24.10
12	252.7	247.6	153.0	468.0	17.15	-1.000	315.0	24.30
13	271.9	267.3	139.0	415.0	19.70	-1.000	276.0	24.40
14	297.8	293.9	117.0	348.0	23.29	-1.000	231.0	24.50
15	305.9	302.2	113.0	333.0	24.47	-1.000	220.0	24.50
16	341.9	333.1	255.0	808.0	9.740	-1.000	553.0	24.80
17	371.8	363.5	254.0	751.0	10.86	-1.000	497.0	24.90
18	385.9	377.8	251.0	726.0	11.34	-1.000	475.0	24.90
19	399.5	391.7	237.0	690.0	11.93	-1.000	453.0	25.00
20	412.5	405.0	227.0	665.0	12.35	-1.000	438.0	25.00
21	436.1	430.8	1.000	640.0	12.78	-1.000	639.0	25.10
22	450.2	443.2	215.0	618.0	13.44	-1.000	403.0	25.10
23	461.9	455.3	206.0	591.0	13.96	-1.000	385.0	25.20
24	473.4	466.9	201.0	571.0	14.63	-1.000	370.0	25.20
25	484.4	478.2	192.0	550.0	15.16	-1.000	358.0	25.20
26	495.0	489.2	184.0	525.0	15.79	-1.000	341.0	25.20
27	505.4	499.7	181.0	509.0	16.44	-1.000	328.0	25.20
28	515.4	509.9	172.0	487.0	17.13	-1.000	315.0	25.30
29	534.5	529.4	160.0	450.0	18.67	-1.000	290.0	25.30
30	552.4	547.7	147.0	409.0	20.53	-1.000	262.0	25.30
31	560.8	556.4	139.0	391.0	21.45	-1.000	252.0	25.40
32	569.3	564.8	137.0	402.0	20.81	-1.000	265.0	25.40
33	588.2	573.1	438.0	1367	5.780	-1.000	929.0	25.40
34	614.7	597.4	510.0	1562	5.140	-1.000	1052	25.40
35	644.2	625.0	574.0	1729	4.670	-1.000	1155	25.40
36	675.9	655.4	615.0	1855	4.360	-1.000	1240	25.50
37	709.6	687.8	653.0	1965	4.090	-1.000	1312	25.40
38	745.5	722.1	687.0	2120	3.750	-1.000	1433	25.30
39	784.4	758.9	753.0	2298	3.490	-1.000	1545	25.20
40	826.5	798.7	818.0	2513	3.200	-1.000	1695	25.10

Note: CTime= Current Time, OxoffT= Air off Time, STime= Start Time, CC= correlation coefficient, SNum= No. of Samples, Temp= Temperature (ºC)

Table A.19: Spiked Raw Data on 11/25/20 (Continued)

Cycle number	CTime (mins)	OxOffT (mins)	STime (secs)	ETime (secs)	Slope (mg/L.hr)	CC	SNum	Temp (ºC)
41	871.9	842.1	870.0	2710	2.930	-1.000	1840	25.00
42	921.5	888.7	947.0	2987	2.640	-1.000	2040	24.90
43	974.5	940.0	1004	3138	2.540	-1.000	2134	24.70
44	1029	993.8	1056	3227	2.480	-1.000	2171	24.60
45	1138	1103	1034	3072	2.660	-1.000	2038	24.60
46	1237	1206	938.0	2735	3.010	-1.000	1797	24.60
47	1325	1298	852.0	2453	3.380	-1.000	1601	24.70
48	1366	1340	805.0	2330	3.540	-1.000	1525	24.90
49	1406	1381	778.0	2236	3.720	-1.000	1458	25.00
50	1444	1419	759.0	2197	3.750	-1.000	1438	25.10

Note: CTime= Current Time, OxoffT= Air off Time, STime= Start Time, CC= correlation coefficient, SNum= No. of Samples, Temp= Temperature (ºC)

APPENDIX F:
SPIKED SAMPLE DATA (15 mL)

Table A.20: Spiked Raw Data on 10/01/2015

Cycle number	CTime (mins)	OxOffT (mins0	STime (secs)	ETime (secs)	Slope (mg/L.hr)	CC	SNum	Temp (ºC)
1	90.10	3.720	3041	7325	1.280	-0.9700	4284	19.00
2	166.9	128.4	1255	3361	2.560	-1.000	2106	20.70
3	211.1	187.1	812.0	2066	3.570	-1.000	1254	21.60
4	244.7	224.1	614.0	1856	4.380	-1.000	1242	22.40
5	274.8	257.8	524.0	1518	5.430	-1.000	994.0	22.90
6	300.2	285.9	432.0	1272	6.440	-1.000	840.0	23.30
7	322.2	309.9	372.0	1099	7.410	-1.000	727.0	23.70
8	359.9	350.2	290.0	873.0	9.290	-1.000	583.0	24.20
9	391.9	383.7	246.0	735.0	11.07	-1.000	489.0	24.50
10	410.0	398.8	240.0	1101	5.900	-0.9800	861.0	24.70
11	595.1	582.1	389.0	1168	6.950	-1.000	779.0	26.00
12	661.0	644.1	341.0	1694	3.680	-0.9900	1353	26.20
13	752.6	720.9	869.0	2932	2.620	-1.000	2063	26.30
14	806.9	772.0	950.0	3242	2.350	-1.000	2292	26.30
15	865.2	828.2	1001	3435	2.230	-0.9900	2434	26.30
16	926.9	887.6	1075	3644	2.090	-0.9900	2569	26.30
17	1054	1014	1094	3719	2.050	-0.9900	2625	26.40
18	1118	1078	1084	3709	2.050	-0.9900	2625	26.30
19	1183	1142	1102	3760	2.030	-0.9900	2658	26.30
20	1248	1207	1113	3862	1.960	-0.9900	2749	26.20
21	1318	1273	1176	4253	1.750	-0.9900	3077	26.00
22	1398	1346	1294	4928	1.480	-0.9900	3634	25.80

Note: CTime= Current Time, OxoffT= Air off Time, STime= Start Time, CC= correlation coefficient, SNum= No. of Samples, Temp= Temperature (ºC)

Table A.21: Spiked Raw Data on 10/14/2015

Cycle number	CTime (mins)	OxOffT (mins)	STime (secs)	ETime (secs)	Slope (mg/L.hr)	CC	SNum	Temp (ºC)
1	2.120	0.030	5.000	246.0	21.67	-0.5500	241.0	20.30
2	34.22	6.450	910.0	2423	3.550	-1.000	1513	21.40
3	68.32	48.65	679.0	1681	5.370	-1.000	1002	22.40
4	93.05	78.45	494.0	1258	7.070	-1.000	764.0	23.10
5	113.5	101.3	416.0	1050	8.500	-1.000	634.0	23.60
6	144.3	137.7	4.000	790.0	10.87	-1.000	786.0	24.40
7	158.4	152.7	1.000	674.0	12.08	-1.000	673.0	24.70
8	173.1	165.8	246.0	628.0	14.10	-1.000	382.0	24.90
9	195.6	189.6	203.0	518.0	17.22	-1.000	315.0	25.40
10	231.7	227.2	153.0	389.0	22.98	-1.000	236.0	25.90
11	239.8	235.6	142.0	361.0	24.64	-1.000	219.0	26.00
12	247.6	243.7	132.0	336.0	26.62	-1.000	204.0	26.10
13	254.9	251.3	124.0	315.0	28.54	-1.000	191.0	26.20
14	262.0	258.6	117.0	296.0	30.30	-1.000	179.0	26.30
15	268.9	265.5	115.0	287.0	31.41	-1.000	172.0	26.40
16	275.7	272.3	111.0	297.0	29.43	-1.000	186.0	26.40
17	287.6	278.9	290.0	754.0	11.62	-1.000	464.0	26.60
18	301.5	293.0	290.0	730.0	12.24	-1.000	440.0	26.80
19	315.0	306.7	289.0	710.0	12.84	-1.000	421.0	26.90
20	327.8	320.0	271.0	667.0	13.64	-1.000	396.0	27.00
21	351.9	344.7	248.0	622.0	14.39	-1.000	374.0	27.20
22	374.9	368.0	240.0	580.0	15.88	-1.000	340.0	27.40
23	385.6	379.1	229.0	551.0	16.75	-1.000	322.0	27.40
24	406.0	399.9	220.0	521.0	17.95	-1.000	301.0	27.60
25	469.3	452.1	579.0	1481	5.970	-1.000	902.0	27.90
26	638.4	593.8	1236	4106	1.850	-0.9900	2870	28.10
27	1282	1243	1269	3385	2.550	-1.000	2116	27.70
28	1386	1351	1120	3032	2.820	-1.000	1912	27.80

Note: CTime= Current Time, OxoffT= Air off Time, STime= Start Time, CC= correlation coefficient, SNum= No. of Samples, Temp= Temperature (ºC)

APPENDIX G:
GLYCEROL PLUS ACCLIMATED MASS

Table A.22: Glycerol plus Acclimated Data on 11/25/2015

Cycle number	CTime (mins)	OxOffT (mins)	STime (secs)	ETime (secs)	Slope (mg/L.hr)	CC	SNum	Temp (ºC)
1	15.38	2.850	0.0000	1504	5.690	-1.000	1504	22.20
2	46.36	29.32	583.0	1462	6.150	-1.000	879.0	22.60
3	89.42	77.20	427.0	1039	8.800	-1.000	612.0	23.40
4	106.5	96.00	364.0	895.0	10.15	-1.000	531.0	23.70
5	121.8	112.42	327.0	800.0	11.41	-1.000	473.0	24.00
6	135.7	127.3	294.0	719.0	12.72	-1.000	425.0	24.30
7	148.2	140.7	259.0	642.0	14.10	-1.000	383.0	24.50
8	158.6	152.7	176.0	529.0	15.31	-1.000	353.0	24.70
9	179.9	173.9	209.0	505.0	18.17	-1.000	296.0	25.00
10	189.5	183.9	199.0	476.0	19.49	-1.000	277.0	25.20
11	198.3	193.3	173.0	426.0	21.21	-1.000	253.0	25.30
12	206.9	202.0	175.0	417.0	22.23	-1.000	242.0	25.40
13	223.1	218.7	157.0	373.0	24.88	-1.000	216.0	25.60
14	230.6	226.5	148.0	354.0	26.31	-1.000	206.0	25.70
15	237.8	233.9	134.0	325.0	28.26	-1.000	191.0	25.80
16	244.7	240.9	135.0	318.0	29.42	-1.000	183.0	25.90
17	257.4	254.3	106.0	266.0	33.72	-1.000	160.0	26.10
18	263.4	260.3	111.0	265.0	34.98	-1.000	154.0	26.10
19	269.4	266.3	108.0	258.0	36.22	-1.000	150.0	26.20
20	274.9	272.1	930.0	238.0	38.29	-1.000	145.0	26.30
21	281.5	277.6	104.0	362.0	20.26	-0.9900	258.0	26.30
22	292.6	284.9	269.0	654.0	14.05	-1.000	385.0	26.50
23	315.9	308.8	247.0	604.0	15.14	-1.000	357.0	26.70
24	326.7	320.2	219.0	559.0	15.90	-1.000	340.0	26.80
25	336.7	330.8	200.0	520.0	16.85	-1.000	320.0	26.90
26	347.1	340.8	221.0	536.0	17.16	-1.000	315.0	27.00
27	357.3	351.0	224.0	532.0	17.31	-1.000	308.0	27.10
28	367.5	361.2	226.0	529.0	17.86	-1.000	303.0	27.10
29	386.5	381.1	184.0	465.0	19.23	-1.000	281.0	27.30
30	395.8	390.1	204.0	473.0	20.03	-1.000	269.0	27.30
31	404.5	399.2	186.0	445.0	20.84	-1.000	259.0	27.40
32	412.9	407.9	180.0	426.0	22.21	-1.000	246.0	27.40
33	420.8	416.2	154.0	399.0	22.06	-1.000	245.0	27.40
34	429.0	424.1	178.0	413.0	22.99	-1.000	235.0	27.40
35	437.0	432.3	174.0	401.0	23.82	-1.000	227.0	27.50
36	459.6	455.4	150.0	353.0	26.64	-1.000	203.0	27.60
37	466.7	462.5	153.0	352.0	27.14	-1.000	199.0	27.60
38	478.9	469.6	224.0	901.0	7.910	-1.000	677.0	27.60
39	502.0	485.7	565.0	1387	6.550	-1.000	822.0	27.70

Note: CTime= Current Time, OxoffT= Air off Time, STime= Start Time, CC= correlation coefficient, SNum= No. of Samples, Temp= Temperature (ºC)

Table A.22: Glycerol plus Acclimated Data on 11/25/2015 (Continued)

Cycle number	CTime (mins)	OxOffT (mins)	STime (secs)	ETime (secs)	Slope (mg/L.hr)	CC	SNum	Temp (ºC)
40	528.7	510.0	640.0	1598	5.640	-1.000	958.0	27.70
41	558.5	537.8	695.0	1781	5.000	-1.000	1086	27.80
42	591.9	568.7	770.0	2020	4.290	-1.000	1250	27.80
43	672.2	642.6	991.0	2567	3.430	-1.000	1576	27.90
44	770.7	735.6	1182	3032	2.940	-1.000	1850	27.70
45	823.5	787.3	1254	3086	2.960	-1.000	1832	27.60
46	1056	1026	1064	2506	3.760	-1.000	1442	27.10
47	1189	1155	1153	2847	3.210	-1.000	1694	27.00

Note: CTime= Current Time, OxoffT= Air off Time, STime= Start Time, CC= correlation coefficient, SNum= No. of Samples, Temp= Temperature (ºC)

Table A.23: Glycerol plus Acclimated Data on 12/03/20

Cycle number	CTime (mins)	OxOffT (mins)	STime (secs)	ETime (secs)	Slope (mg/L.hr)	CC	SNum	Temp (°C)
1	67.11	3.030	513.0	7177	1.100	-0.5900	6664	18.80
2	156.0	124.6	1000	2768	3.050	-1.000	1768	20.90
3	240.3	228.7	332.0	1055	7.440	-1.000	723.0	23.50
4	259.5	248.7	342.0	953.0	8.900	-1.000	611.0	23.90
5	276.3	266.9	293.0	828.0	10.19	-1.000	535.0	24.30
6	290.7	282.9	235.0	699.0	11.55	-1.000	464.0	24.60
7	315.8	309.5	182.0	568.0	13.95	-1.000	386.0	25.10
8	326.6	321.1	151.0	505.0	15.15	-1.000	354.0	25.30
9	336.8	331.6	146.0	478.0	16.43	-1.000	332.0	25.50
10	347.2	341.8	163.0	470.0	17.62	-1.000	307.0	25.70
11	356.5	351.8	133.0	421.0	18.74	-1.000	288.0	25.80
12	364.6	360.7	95.00	366.0	19.87	-1.000	271.0	25.90
13	372.4	368.7	98.00	343.0	21.54	-1.000	245.0	26.00
14	381.0	376.9	133.0	369.0	22.84	-1.000	236.0	26.20
15	396.4	392.9	101.0	311.0	25.63	-1.000	210.0	26.30
16	403.5	400.3	90.00	292.0	26.86	-1.000	202.0	26.40
17	409.6	407.0	62.00	253.0	28.39	-1.000	191.0	26.50
18	416.2	413.3	80.00	264.0	29.23	-1.000	184.0	26.60
19	422.7	419.8	81.00	261.0	30.03	-1.000	180.0	26.60
20	429.9	426.5	106.0	304.0	27.4	-1.000	198.0	26.70
21	441.9	433.6	251.0	744.0	11.02	-1.000	493.0	26.80
22	480.8	473.9	204.0	630.0	12.69	-1.000	426.0	27.20
23	493.4	486.2	224.0	636.0	13.21	-1.000	412.0	27.30
24	504.2	498.4	152.0	550.0	13.49	-1.000	398.0	27.30
25	514.2	508.9	117.0	518.0	13.56	-1.000	401.0	27.40
26	526.1	519.4	214.0	593.0	14.26	-1.000	379.0	27.50
27	536.2	530.8	140.0	508.0	14.78	-1.000	368.0	27.50
28	546.5	540. 9	171.0	509.0	15.95	-1.000	338.0	27.60
29	556.9	551.1	184.0	514.0	16.32	-1.000	330.0	27.60
30	565.8	561.1	123.0	444.0	16.86	-1.000	321.0	27.60
31	575.3	570.2	159.0	461.0	17.83	-1.000	302.0	27.70
32	584.1	579.4	138.0	427.0	18.68	-1.000	289.0	27.70
33	593.2	588.2	162.0	433.0	19.81	-1.000	271.0	27.70
34	602.2	597.2	163.0	430.0	20.31	-1.000	267.0	27.80
35	610.2	605.8	88.00	434.0	16.43	-0.9900	346.0	27.80
36	659.6	640.6	590.0	1687	4.890	-1.000	1097	27.80
37	724.3	701.4	674.0	2071	3.870	-1.000	1397	27.90
38	806.1	7772	872.0	2604	3.080	-1.000	1732	27.90
39	1082	1045	1122	3354	2.390	-0.9900	2232	27.60

Note: CTime= Current Time, OxoffT= Air off Time, STime= Start Time, CC= correlation coefficient, SNum= No. of Samples, Temp= Temperature (°C)

Table A.23: Glycerol plus Acclimated Data on 12/03/20 (Continued)

Cycle number	CTime (mins)	OxOffT (mins)	STime (secs)	ETime (secs)	Slope (mg/L.hr)	CC	SNum	Temp (ºC)
40	1191	1157	1018	3011	2.700	-1.000	1993	27.30
41	1233	1209	1.000	2883	3.070	-0.9900	2882	27.20
42	1336	1306	873.0	2760	2.840	-1.000	1887	27.20
43	1384	1354	853.0	2851	2.690	-0.9900	1998	27.30

Note: CTime= Current Time, OxoffT= Air off Time, STime= Start Time, CC= correlation coefficient, SNum= No. of Samples, Temp= Temperature (ºC)

APPENDIX H:
GLYCEROL EFFECT

Table A.24: Glycerol Effect Data on 09/01/2015

CTime (hrs)	Slope With Glycerol (mg/L.hr)	Slope W/O Glycerol (mg/L.hr)	Glycerol Effect (mg/L.hr)
0.764	2.26	-	-
1.67	4.19	-	-
2.24	5.57	-	-
2.28	-	1.57	-
2.65	6.8	2.11	4.68
2.99	7.99	2.63	5.36
3.25	8.97	3.01	5.95
3.35	-	3.16	-
3.56	8.09	3.66	4.43
3.98	-	4.64	-
4.11	4.18	5.01	-0.83
4.45	-	5.98	-
4.64	4.78	6.24	-1.46
4.83	-	7.26	-
5.04	4.88	8.05	-3.17
5.45	-	9.63	-
5.56	5.03	8.52	-3.49
5.73	-	6.97	-
5.96	5.41	5.44	-0.027
6.31	-	3.03	-
6.40	5.65	2.98	2.66
6.88	5.83	2.75	3.07
7.23	-	2.58	-
7.28	6.2	2.58	3.62
7.60	6.69	2.58	4.11
7.97	7.08	2.58	4.5
8.08	-	2.58	-
8.32	7.43	2.57	4.85
8.69	7.59	2.57	5.01
8.84	-	2.57	-
9.01	7.92	2.52	5.39
9.28	8.32	2.45	5.87
9.62	8.47	2.35	6.12
9.88	8.85	2.28	6.56
9.88	-	2.28	-
10.2	9.04	2.28	6.76
10.5	9.4	2.28	7.12
10.7	-	2.28	-
10.7	9.75	2.27	7.47
10.9	10.1	2.22	7.92

Table A.24: Glycerol Effect Data on 09/01/2015 (Continued)

CTime (hrs)	Slope WithGlyc (mg/L.hr)	Slope W/O Glyc (mg/L.hr)	Glycerol Effect (mg/L.hr)
11.2	10.6	2.14	8.48
11.5	11.0	2.07	8.93
11.7	11.2	2.01	9.21
11.8	-	2.00	-
11.9	11.0	1.93	9.13
12.4	3.84	1.78	2.05
13.2	2.97	1.48	1.48
13.2	-	1.47	-
13.9	2.83	1.36	1.47
14.7	-	1.25	-
14.8	2.76	1.24	1.52
15.6	2.67	1.17	1.49
16.3	-	1.12	-
16.6	2.81	1.15	1.66
17.4	3.07	1.23	1.84
17.9	-	1.28	-
18.3	3.08	1.28	1.79
19.2	2.76	1.29	1.46
19.5	-	1.30	-
20.0	2.93	1.32	1.60
21.0	-	1.38	-
21.3	2.47	1.40	1.06
21.7	2.5	1.44	1.06
22.4	-	1.49	-
22.7	1.89	-	-

Note: CTime= Current Time

Table A.25: Glycerol Effect Data on 09/02/2015

CTime (hrs)	Slope WithGlyc (mg/L.hr)	Slope W/O Glyc (mg/L.hr)	Glycerol Effect (mg/L.hr)
0.564	2.28		
1.39		2.26	
1.57	3.57	2.56	1.01
2.07		3.41	
2.15	4.76	3.54	1.22
2.53	5.84	4.27	1.57
2.75		4.68	
2.93	6.86	5.12	1.75
3.19		5.77	
3.31	8.02	6.13	1.88
3.56		6.89	
3.66	4.8	7.27	-2.47
3.83		7.97	
4.16		8.84	
4.24	3.4	7.85	-4.45
4.70		2.17	
4.91	3.71	2.14	1.57
5.54	3.82	2.05	1.77
5.69		2.03	
6.14	4.17	2.18	1.98
7.07		1.61	
7.26	4.48	1.58	2.89
7.85	4.51	1.50	3.00
8.28	4.84	1.44	3.39
8.45		1.42	
8.78	5.01	1.40	3.60
9.25	5.19	1.37	3.82
9.78	5.3	1.34	3.96
9.95		1.33	
11.0	6.17	1.10	5.063
11.3	6.65	1.04	5.60
11.7	7.01	0.966	6.04
11.7		0.96	
12.0	7.49	0.98	6.50
12.3	7.87	1.00	6.86
12.7	8.22	1.03	7.18
12.9	8.78	1.05	7.72
13.2	9.15	1.08	8.06
13.4	9.7	1.10	8.59
13.7	9.85	1.12	8.73
13.9	9.42	1.14	8.28

Table A.25: Glycerol Effect Data on 09/02/2015 (Continued)

CTime (hrs)	Slope With Glyc (mg/L.hr)	Slope W/O Glyc (mg/L.hr)	Glycerol Effect (mg/L.hr)
14.6	2.57	1.19	1.37
14.9	0.000	1.21	-1.21
15.5	2.59	1.26	1.32
16.6	2.72	1.35	1.36
17.4	2.81	1.42	1.38
18.3	2.96	1.48	1.47
19.2	2.85	1.56	1.28
20.0	2.46	1.63	0.83
21.3	2.38	1.73	0.64
21.7	1.76	1.76	-0.007
22.7	1.35	1.85	-0.500

Note: CTime= Current Time

Table A.26: Glycerol Effect Data on 09/24/2015

CTime (hrs)	Slope WithGlyc (mg/L.hr)	Slope W/O Glyc (mg/L.hr)	Glycerol Effect (mg/L.hr)
0.37	-	4.65	-
0.48	3.59	4.85	-1.26
0.84	-	5.52	-
0.95	4.69	5.78	-1.09
1.24	-	6.43	-
1.49	5.73	6.98	-1.25
1.60	-	7.23	-
1.88	6.89	8.00	-1.11
1.94	-	8.15	-
2.23	7.97	9.11	-1.14
2.24	-	9.15	-
2.51	-	10.1	-
2.53	9.06	10.2	-1.13
2.75	9.95	11.0	-1.10
2.76	-	11.1	-
3.00	10.9	11.8	-0.935
3.00	-	11.8	-11.8
3.26	12.0	8.02	4.05
3.27	-	8.01	-
3.45	12.3	6.42	5.85
3.54	0	5.60	-5.60
3.73	-	3.99	-
3.75	5.89	3.98	1.91
4.25	-	3.74	-
4.41	3.47	3.65	-0.18
4.92	-	3.39	-
5.11	3.24	3.31	-0.075
5.72	-	3.09	-
5.83	3.44	3.07	0.365
6.37	-	3	-
6.50	3.68	2.92	0.760
7.15	3.92	2.54	1.377
7.30	-	2.45	-
7.76	4.23	2.34	1.88
7.94	0	2.30	-2.30
8.14	-	2.26	-
8.31	4.76	1.95	2.81
8.81	5.3	1.04	4.25
9.18	5.95	0.37	5.57
9.42	-	1.66	-
9.67	6.71	1.62	5.09

Table A.26: Glycerol Effect Data on 09/24/2015 (Continued)

CTime (hrs)	Slope WithGlyc (mg/L.hr)	Slope W/O Glyc (mg/L.hr)	Glycerol Effect (mg/L.hr)
10.0	7.58	1.55	6.02
10.3	8.46	1.50	6.96
10.6	-	1.45	-
10.6	9.42	1.45	7.97
10.8	10.0	1.40	8.59
11.2	11.6	1.35	10.3
11.4	12.8	1.31	11.5
11.5	13.3	1.28	11.9
11.8	15.6	1.24	14.3
11.9	16.6	1.20	15.4
12.0	-	1.20	-
12.3	2.15	1.12	1.02
13.7	1.14	0.837	0.30
14.5	-	0.680	-
15.6	1.04	0.596	0.44
16.5	2.16	0.527	1.63
17.0	2.20	0.488	1.71
17.6	2.18	0.450	1.73
17.6	-	0.450	-
18.0	2.34	0.416	1.92
18.5	2.38	0.384	1.99
19.0	1.89	0.346	1.54
19.7	1.68	0.300	1.38
20.4	1.62	0.247	1.37
21.1	1.99	0.198	1.79
22.6	0.540	0.088	0.452

Note: CTime= Current Time

Table A.27: Glycerol Effect Data on 09/25/2015

CTime (hrs)	Slope WithGlyc (mg/L.hr)	Slope W/O Glyc (mg/L.hr)	Gly Effect (mg/L.hr)
0.853	-	2.33	-
1.09	2.50	2.68	-0.184
1.71	-	3.61	-
1.73	3.97	3.63	0.338
2.23	-	4.42	-
2.38	5.19	4.69	0.504
2.82	6.15	5.44	0.712
2.85	-	5.49	-
3.19	7.18	6.282	0.897
3.28	-	6.48	-
3.53	8.13	6.88	1.24
3.59	-	7	-
4.01	-	7.82	-
4.26	3.66	5.44	-1.78
4.54	-	2.69	-
4.86	4.1	2.69	1.41
5.44	4.05	2.69	1.36
5.56	-	2.69	-
6.01	4.19	2.59	1.59
6.49	-	2.5	-
6.56	4.30	2.49	1.80
7.10	4.33	2.43	1.89
7.45	-	2.4	-
7.57	4.55	2.44	2.11
8.20	4.37	2.64	1.73
8.47	-	2.25	-
8.73	4.4	2.17	2.22
9.18	4.73	2.05	2.67
9.60	-	1.94	-
9.78	4.61	1.88	2.72
10.9	-	1.58	-
12.5	-	1.26	-
12.7	7.97	1.23	6.74
13.0	8.72	1.17	7.54
13.3	9.56	1.13	8.42
13.6	10.2	1.09	9.11
13.8	10.0	1.06	8.94
14.4	2.57	0.983	1.58
14.4	-	0.980	-
15.4	2.10	0.863	1.23
15.6	1.74	0.832	0.908

Table A.27: Glycerol Effect Data on 09/25/2015 (Continued)

CTime (hrs)	Slope WithGlyc (mg/L.hr)	Slope W/O Glyc (mg/L.hr)	Gly Effect (mg/L.hr)
16.6	1.92	0.721	1.19
16.9	-	0.68	-
17.0	1.76	0.674	1.08
17.6	1.75	0.654	1.09
18.0	1.7	0.637	1.06
18.5	1.59	0.620	0.969
20.1	-	0.560	-

Note: CTime= Current Time

Table A.28: Glycerol Effect Data on 09/28/2015

CTime (hrs)	Slope WithGlyc. (mg/L.hr)	Slope W/O Glyc. (mg/L.hr)	Glycerol Effect (mg/L.hr)
1.70	1.5	-	-
1.90	-	1.54	-
2.81	-	3.19	-
2.90	2.89	3.27	-0.380
3.59	-	4.76	-
3.65	4.03	4.83	-0.800
4.05	-	6.11	-
4.22	5.08	6.34	-1.26
4.44	-	7.34	-
4.68	5.95	7.70	-1.76
4.77	-	8.41	-
5.07	-	9.66	-
5.09	6.85	9.69	-2.84
5.30		10.5	
5.45	7.81	9.62	-1.80
5.77	8.90	6.45	2.45
5.82	-	2.43	-
6.06	9.67	2.46	7.20
6.56	2.58	2.59	-0.009
6.68	-	2.69	-
7.55	2.93	2.59	0.333
7.54	-	2.53	-
8.42	-	2.58	-
9.05	3.56	2.55	1.00
9.29	-	2.51	-
9.70	3.92	2.50	1.41
10.0	-	2.5	-
10.3	4.34	2.47	1.86
10.8	4.84	2.32	2.51
11.1	-	2.08	-
11.3	5.51	2.07	3.43
11.8	6.14	2.04	4.09
12.1	6.9	1.98	4.91
12.5	7.39	1.85	5.4
12.6	-	1.41	-
13.1	9.43	1.40	8.02
13.4	10.4	1.40	9.03
13.6	11.3	1.38	9.96
13.9	12.4	1.33	11.0
14.2	-	1.12	-

Table A.28: Glycerol Effect Data on 09/28/2015 (Continued)

CTime (hrs)	Slope With Glyc. (mg/L.hr)	Slope W/O Glyc. (mg/L.hr)	Glycerol Effect (mg/L.hr)
14.3	2.77	1.12	1.65
15.4	1.51	1.12	-
15.9	-	1.12	-
17.0	1.32	1.06	0.261
18.3	-	0.88	-
20.6	1.15	0.937	0.213
22.5	1.17	1.04	0.127

Note: CTime= Current Time

Table A.29: Glycerol Effect Data on 09/29/2015

C Time (hrs)	Slope With Glyc. (mg/L.hr)	Slope W/O Glyc. (mg/L.hr)	Glycerol Effect (mg/L.hr)
0.418	-	3.48	-
0.499	3.42	3.58	-0.158
1.10	-	4.31	-
1.11	4.57	4.34	0.232
1.59	5.83	5.27	0.558
1.93	7.01	5.92	1.09
2.20	-	6.45	-
2.33	8.34	6.67	1.66
2.59	-	7.17	-
2.62	9.47	7.25	2.21
2.89	10.6	8.12	2.51
2.95	-	8.32	-
3.09	11.5	8.67	2.80
3.56	-	9.82	-
3.95	-	4.15	-
4.00	4.71	4.06	0.65
4.49	5.12	3.33	1.79
4.67	-	3.05	-
4.95	5.24	3.04	2.12
5.40	5.34	3.03	2.30
5.48	-	3.03	-
5.84	5.57	2.95	2.62
6.26	5.75	2.85	2.90
6.30	-	2.84	-
6.62	6.17	2.80	3.36
7.07	6.23	2.76	3.47
7.16	-	2.75	-
7.40	6.70	2.72	3.98
7.83	6.80	2.67	4.12
8.07	-	2.65	-
8.18	7.15	2.65	4.49
8.52	7.49	2.68	4.81
8.84	-	2.7	-
8.85	7.92	2.67	5.22
9.16	8.22	2.64	5.58
9.25	-	2.62	-
9.46	8.76	2.58	6.17
9.74	9.30	2.53	6.77
9.95	-	2.49	-
10.0	9.87	2.47	7.39
10.3	10.5	2.41	8.07

Table A.29: Glycerol Effect Data on 09/29/2015 (Continued)

C Time (hrs)	Slope With Glyc. (mg/L.hr)	Slope W/O Glyc. (mg/L.hr)	Glycerol Effect (mg/L.hr)
10.5	11.1	2.36	8.74
10.7	11.7	2.30	9.46
10.9	12.4	2.24	10.1
10.9	-	2.24	-
11.2	11.8	2.18	9.61
11.5	3.96	2.08	1.87
12.1	-	1.95	-
12.2	3.56	1.93	1.63
13.0	3.12	1.75	1.37
13.4	-	1.67	-
14.4	3.17	1.63	1.54
14.8	-	1.61	-
15.3	2.92	1.62	1.30
15.9	3.13	1.62	1.50
16.2	-	1.63	-
17.5	3.00	1.69	1.31
17.6	-	1.69	-
18.5	2.60	1.66	0.935
18.9	-	1.65	-
19.4	2.36	1.61	0.750
19.6	0.37	1.58	-1.20
18.9	2.12	1.65	0.47
20.4	-	1.5	-
21.3	2.09	1.43	0.659
22.0	-	1.37	-
22.6	1.59	1.41	0.180

Note: CTime= Current Time

Table A.30: Glycerol Effect Data on 10/01/2015

CTime (hrs)	Slope WithGlyc (mg/L.hr)	Slope W/O Glyc (mg/L.hr)	Glycerol Effect (mg/L.hr)
1.11	-	1.66	-
1.50	1.28	2.18	-0.902
2.04	-	2.91	-
2.78	2.56	3.95	-1.39
2.85	-	4.05	-
3.32	-	4.95	-
3.52	3.57	5.39	-1.82
3.85	-	6.13	-
4.07	4.38	6.69	-2.32
4.26	-	7.14	-
4.58	5.43	8.23	-2.79
4.66	-	8.49	-
4.99	-	9.26	-
5.37	7.41	10.2	-2.76
5.38	-	10.19	-
5.65	8.11	7.15	0.963
5.89	-	4.48	-
5.99	9.29	4.49	4.80
6.24	9.98	4.51	5.47
6.48	-	4.53	-
6.53	11.07	4.51	6.56
6.84	5.90	4.39	1.50
7.19	-	4.26	-
7.24	4.67	4.24	0.425
7.74	5.09	4.06	1.02
8.21	5.39	3.89	1.49
8.66	5.58	3.74	1.84
9.09	5.98	3.58	2.39
9.49	6.42	3.45	2.97
9.50	-	3.44	-
9.92	6.95	3.59	3.36
10.2	7.37	3.70	3.67
10.5	7.75	3.82	3.93
11.0	3.68	3.99	-0.308
11.6	3.07	4.20	-1.13
12.5	2.62	4.54	-1.92
13.4	2.35	4.87	-2.52
14.4	2.23	5.22	-2.99
15.4	2.09	5.60	-3.50
16.3	2.23	5.92	-3.69
17.6	2.05	6.36	-4.31

Table A.30: Glycerol Effect Data on 10/01/2015 (Continued)

CTime (hrs)	Slope With Glyc (mg/L.hr)	Slope W/O Glyc (mg/L.hr)	Glycerol Effect (mg/L.hr)
18.6	2.05	6.75	-4.70
19.7	2.03	7.14	-5.10
20.8	1.96	7.53	-5.57
21.9	1.75	7.96	-6.20
23.3	1.48	8.43	-6.95

Note: CTime= Current Time

Table A.31: Glycerol Effect Data on 10/14/2015

CTime (hrs)	Slope WithGlyc (mg/L.hr)	Slope W/O Glyc (mg/L.hr)	Glycerol Effect (mg/L.hr)
0.418	-	3.48	-
0.500	3.42	3.58	-0.159
1.10	-	4.31	-
1.11	4.57	4.33	0.232
1.60	5.83	5.27	0.558
1.93	7.01	5.92	1.09
2.20	-	6.45	-
2.33	8.34	6.68	1.66
2.60	-	7.17	-
2.62	9.47	7.26	2.21
2.88	10.6	8.12	2.51
2.95	-	8.32	-
3.09	11.5	8.67	2.80
3.57	-	9.82	-
3.95	-	4.15	-
4.00	4.71	4.06	0.645
4.49	5.12	3.33	1.79
4.67	-	3.05	-
4.95	5.24	3.04	2.19
5.40	5.34	3.03	2.30
5.48	-	3.03	-
5.84	5.57	2.95	2.63
6.27	5.75	2.85	2.90
6.30	-	2.84	-
6.62	6.17	2.80	3.36
7.07	6.23	2.76	3.47
7.16	-	2.75	-
7.40	6.70	2.72	3.97
7.83	6.80	2.68	4.12
8.07	-	2.65	-
8.19	7.15	2.66	4.49
8.52	7.49	2.68	4.81
8.84	-	2.70	-
8.85	7.92	2.70	5.22
9.16	8.22	2.64	5.58
9.25	-	2.62	-
9.46	8.76	2.58	6.18
9.75	9.30	2.53	6.77
9.95	-	2.49	-
10.0	9.87	2.47	7.39

Table A.31: Glycerol Effect Data on 10/14/2015 (Continued)

CTime (hrs)	Slope WithGlyc (mg/L.hr)	Slope W/O Glyc (mg/L.hr)	Glycerol Effect (mg/L.hr)
10.3	10.5	2.41	8.07
10.5	11.1	2.36	8.74
10.7	11.7	2.30	9.45
10.9	12.4	2.24	10.2
10.9	-	2.24	-
11.2	11.8	2.18	9.62
11.5	3.96	2.08	1.87
12.1	-	1.95	-
12.2	3.56	1.92	1.63
13.0	3.12	1.75	1.37
13.4	-	1.67	-
14.4	3.17	1.63	1.54
14.8	-	1.61	-
15.3	2.92	1.62	1.30
15.9	3.13	1.63	1.50
16.2	-	1.63	-
17.5	3.00	1.69	1.31
17.6	-	1.69	-
18.5	2.60	1.66	0.935
18.9	-	1.65	-
19.4	2.36	1.61	0.750
19.7	0.37	1.58	-1.21
18.9	2.12	1.65	0.47
20.4	-	1.5	-
21.3	2.09	1.43	0.660
22.0	-	1.37	-
22.7	1.59	1.41	0.180

Note: CTime= Current Time

APPENDIX I:
WASTEWATER CHARACTERISTICS

Table A.32: Wastewater Characteristics

Influent Date	pH	VFA (mg COD/L)	TP (mg P/L)	TN (mg N/L)
9/3/2015	7.00	21.0	5.30	36.2
9/23/2015	7.50	0.000	4.50	36.7
9/29/2015	7.50	0.000	4.60	38.2
10/1/2015	7.50	0.000	1.90	26.8
10/13/2015	7.50	0.000	5.20	-
11/25/2015	7.50	0.000	5.50	38.1
12/3/2015	7.50	0.000	5.80	37.5

Table A.33: Phase I RBCOD Data

	(Un-spike)	(Spike)		
		(Peak A)	(Peak B)	(Glycerol Effect)
No of Sample	rbcod (mg COD/L)	rbcod (sp 1) (mg COD/L)	rbcod (sp 2) (mg COD/L)	rbcod (Δ) (mg COD/L)
9/1/2015	48.1	30.6	140	98.0
9/2/2015	40.0	24.1	143	114
9/24/2015	56.7	58.6	127	92.4
9/25/2016	38.0	35.0	128	84.3
9/28/2015	49.2	54.0	106	60.0
9/29/2015	39.5	49.2	129	87.0

Table A.34: Phase II RBCOD Data

	(Un-spike)	(Spike)		
		(Peak A)	(Peak B)	(Glycerol Effect)
No of Sample	rbcod (mg COD/L)	rbcod (sp 1) (mg COD/L)	rbcod (sp 2) (mg COD/L)	rbcod (Δ) (mg COD/L)
10/1/2015	67.5	55.6	66.4	25.0
10/14/2015	80.5	114	107	85.6

Table A.35: Phase III RBCOD Data

		Glycerol	Primary solid +	Glycerol
	(Peak A)	(Peak B)	(Peak A')	(Peak B')
No of Sample	rbcod (sp 1) (mg COD/L)	rbcod (sp 2) (mg COD/L)	rbcod (sp 1) (mg COD/L)	rbcod (sp 2) (mg COD/L)
11/25/2015	124	187	152	208
12/3/2015	100	146	99.0	172

REFERENCES

Barbirato, F., Chedaille, D., and Bories, A., 1997. Propionic acid fermentation from glycerol: comparison with conventional substrates. Applied Microbiology Biotechnology, 47, 441-446.

Barnard, J.L., and Abraham, K., 2006. Key features of successful BNR operation. Water Science and Technology, 53, 1-9.

Bodik, I., Blstakova, A., Sedlacek, S., and Hutnan, M., 2009. Biodiesel waste as source of organic carbon for municipal WWTP denitrification. Bioresource Technology, 100, 2452-2456.

Bondioli, P., and Bella, L.D., 2005. An alternative spectrophotometric model for the determination of free glycerol in biodiesel. European Journal of Lipid Science and Technology, 107, 153-157.

Bories, A., Himmi, E.H., Jauregul, J.A., and Gonzales, V.A., 2003. Glycerol fermentation with propionibacteria and optimisation of the production of propionic acid. Science Des Aliments, 24.2, 121-135.

Boulineau, S., Tostevin, F., Kiviet, D.J., Wolde, P.R.t., Nghe, P., and Tans, S.J., 2013. Single-cell dynamics reveals sustained growth during diauxic shifts. PLoS ONE 8(4): e61686. doi:10.1371/journal.pone.0061686.

Broughton, A., Pratt, S., and Shilton, A., 2008. Enhanced biological phosphorus removal for high-strenght wastewater with a low rbcod:p ratio. Bioresource Technology, 99, 1236–1241.

Chaudhary, N., 2010. Anaerobic fermentation of glycerol by Escherichia coli K12 for the production of ethanol. Research in partial fulfillment of degree of Master in science, McGill University, Montreal, Quebec, Canada

Chaudhary, N., Ngadi, M.O., Simpson, B.K and Kassama, L.S., 2011. Biosynthesis of ethanol and hydrogen by glycerol fermentation using *Escherichia coli.* Advances in Chemical Engineering and Science, 1, 83-89.

Cho, E., and Molof, H.A., 2004. Effect of sequentially combining methanol and acetic acid on the performance of biological nitrogen and phosphorus removal. Journal of Environmental Management, 73, 183-187.

Chu, A., Mavinic, D,S., Kelly, H.G., and Ramey, W.D., 1994. Volatile fatty acid production in thermophilic aerobic digestion of sludge. Water Resource, 28, 1513-1522.

Clayton, J.A., Ekama, G.A, Wentzel, M.C., and Maris, G.V.R., 1991. Denitrification kinetics in biological nitrogen and phosphorus removal activated sludge systems treating municipal wastewaters. Water Science Technology, 23, 1025-1035.

Clomburg, J.M., and Gonzalez, R., 2013. Anaerobic fermentation of glycerol: a platform for renewable fuels and chemicals. Trends Biotechnology, 31, 20-28.

Coats, E.R., Dobroth, Z.T., and Brinkman, C.K., 2015. EBPR using crude glycerol: assessing process resiliency and exploring metabolic anomalies. Water Environment Resource, 87, 68-79.

Cyplik, P., Juzwa, W., Marecik, R., Czarny, P.J., Cyplik, P.A., Czarny, J., Drozdzynska, R., and Chrzanowski, L., 2013. Denitrification of industrial wastewater: Influence of glycerol addition on metabolic activity and community shifts in a microbial consortium. Chemosphere, 93, 2823-2831.

Danesh, S., and Oleszkiewicz J.A., 1997. Volatile fatty acid production and uptake in biological nutrient removal systems with process separation. Water Environment Resource, 69, 1106-1111.

Dauknys, R., Vaboliene, G., Valentukeviciene, M., and Rimeika, M., 2009. Influence of substrate on biological removal of phosphours. Ekologija, 55, 220-225.

Demirbas, A., 2009. Biofuels: Securing the Planet's Future Energy Needs. Green Energy and Technology, pp-162.

Dharmadi, Y., A. Murarka., and R. Gonzalez., 2006. Anaerobic fermentation of glycerol by *Escherichia coli*: a new platform for metabolic engineering. Biotechnology and Bioengineering. 94, 821-829.

Drewnoswski, J., 2014. The impact of slowly biodegradable organic compounds on the oxygen uptake rate in activated sludge systems. Water Science Technology, 69, 1136-1144.

Drozdzynska, A., Pawlicka, J., Kubiak, P., Kosmider, A., Pranke, D., Schmidt, A.O., and Czaczyk, K., 2014. Conversion of glycerol to 1.3-propanediol by *Citrobacter freundii* and *Hafnia alvei*- newly isolated strains from the Enterobaceteriaceae. New Biotechnology, 31, 402-410.

Ekama, G.A., and Marais, G.v.R., 1979. Dynamic behavior of the activated sludge process. Water pollution control federation Part I, 51, 534-556.

Ekama, G.A., Siebritz, I.P., and Marais, G.V., 1983. Considerations in the process design of nutrient removal activated sludge process. Water Science and Technology, 15, 283-318.

Foglar, L., and Briski, F., 2003. Wastewater denitrification process- the influence of methanol and kinetic analysis. Process Biochemistry, 39, 95-103.

Gong, L., Huo, M., Yang, Q., Li, J., Ma, B., Zhu, R., Wang, S., and Peng, Y., 2013. Performance of heterotrophic partial denitirification under feast-famine condition of electron donor: A case study using acetate as external carbon source. Bioresource Technology, 133, 263-269.

Gu, A.Z., Saunders, A., Neethling, J.B., Stensel, H.D., and Blackall, L.L., 2008. Functionally relevant microorganisms to enhanced biological phosphours removal performance at full-scale wastewater treatment plants in the Unites States. Water Environment Resource, 80, 688-698.

Guerrero, J., Taya, C., Guisasola, A., and Baeza J.A., 2012 Glycerol as a sole carbon source for enhance biological phosphorus removal. Water Research, 46, 2983-2991.

Gupta, A., Murarka, A., Campbell, P., and Gonzalez, R., 2009. Anaerobic fermentation of glycerol in *Paenibacillus macerans*: metabolic pathways and environmental determinants. Applied and Environmental Microbiology, 75, 5871-5883.

Hinojosa, J., Riffat, R., Fink, S., Murthy, S., Selock, K., Bott, C., Takacs, I., Dold, P., and Wimmer, (2008). *Estimating the Kinetics and Stoichiometry of Heterotrophic Denitrifying Bacteria with Glycerol as an External Carbon Source*. Proceedings of the Water Environment Federation, WEFTEC, Session 1-10, 274-288.

Her, J. J., and Huang, J.S., 1995 Influence of carbon source and C/N ratio on nitrate/nitrite denitrification and carbon breakthrough. Bioresource Technology, 54, 45-51.

Henz, M.P., Harremoes, J, la C., and Janse E.A, 2001. Wastewater treatment biological and chemical processes. 3rd edn: Springer Verlag. pp-436.

Henz, M., Loosdrecht, M.CM.v., Ekama, G.A., and Brdjanovic, D., 2008. Biological wastewater treatment: Principle, Modeling and design pp-82, 115.

Himmi,E.H., Bories, A., Boussaid, A., and Hassani, L., 2000. Propionic acid fermentation of glycerol and glucose by *Propionibacterium acidipropionici* and *Propionibacterium freudenreichii* ssp. *Shermanii*. Applied Microbiol Biotechnology, 53, 435-440.

Hu, Z.R., Wentzel, M., and Ekama, G.A., 2002. The significance of denitrifying polyphosphate accumulating organisms in biological nutrient removal activated sludge systems. Water Science Technology. 46, 129-138.

Janssen, P.M.J., Roest, H.F.V., and Eggers, E., 1996. The Carrousel and the Carrousel-2000 systems: A guarantee for total nutrient removal. European Water Pollution Control, 6, 10-16.

Jeon, C.O., and Park, J.M., 2000. Enhanced biological phosphours removal in a sequencing batch reactor supplied with glucose as a sole carbon source. Water Resource, 34, 2160-2170.

Katarzyna, B., Dorota, K., and Karol, Z., 2015. Glycerine as a carbon source in nitrite removal and sludge production. Chemical Engineering Journal, 267, 324-331.

Kosimider, A., Drozdzynska, A., Blaszka, K., Leja, K., and Czaczyk, K. 2010. Propionic acid production by *Propionibacterium freudenreichii* ssp. *shermanii* using crude glycerol and whey lactose industrial wastes. Polish Journal of Environmental Studies, 19, 1249-1253.

Kuai, L., and Verstraete, W., 1999. Autotrophic denitrification with elemental sulphur in small-scale wastewater treatment facilities. Environmental Technology, 20, 201-209.

Lee, D.U., Lee, I.S., Choi, Y.D., and Bae, J.H., 2001. Effects of external carbon source and empty bed contact time on simultaneous heterotrophic and sulfur-utilizing autotrophic denitrification. Process Biochemistry, 36, 1215-1224.

Liu, Y., Zhang, Y.G., Zhang, R.B., Zhang, F., and Zhu, J., 2011. Glycerol/Glucose Co-Fermentation: One More Proficient Process to produce Propionic Acid by *Propionibacterium acidipropionici*. Current Microbiology, 62, 152–158.

Melidis, P., and Tseles, D., 2009 Nitrogen removal from landfill leachate by addition of biodiesel glycerol waste as external carbon source. Proceedings of the 11th International conference on Environmental Science and Technology, A 916-922

Metcalf and Eddy Inc., Tchobanoglous, G., Stensel, H.D., and Burton, F., 2013. Wastewater engineering treatment and reuse (5th ed.) Mc Graw Hill Higher Education. pp-874, ISBN: 0073401188.

Marais, G.V.R., and Ekama, G.A., 1976. The activated sludge process, Part 1: Steady state behaviour. Water SA, 2, 163–200.

Naidoo, V., 1997. Municipal wastewater characterization-Application of denitrification batch tests. Academic requirement for the degree of Doctor of Philosophy University of Natal, Durban.

Naidoo, V., Urbain, V., Ginestet, P., and Buckley, C.A., 2000. Reliability of the anoxic respirometeric technique for wastewater characterization using EBPR and non-EBPR sludge. Water Institute for Southern African Biennial Conference, Sun City, South Africa, May 28-June 1, Water Institute for Southern Africa; Midrand, South Africa.

Oehmen, A., Lemos, P.C., Carvalho, G., Yuan, Z., Keller, J., Blackall, L.L., and Reis, M.A.M., 2007. Advances in enhanced biological phophours removal: From micro to macro scale. Water Research, 41, 2271-2300.

Oehmen, A., Saunders, A.M., Vives, M.T., Yuan, Z., and Keller, J., 2006. Competition between polyphosphate and glycogen accumulating organisms in enhanced biological phosphorus removal systems with acetate and propionate as carbon sources. Journal of Biotechnology, 123, 22-32.

Orhon, D., Okutman D., and Insel, G., 2002. Characterisation and biodegrdation of settleable organic matter for domestic wastewater. Water SA, 28, 299-306.

Pagliaro, M., and Rossi, M., 2008. The future of glycerol: new uses of a versatile raw material. RSC green chemistry book series, pp- 1-17.

Papanikolaous, S., Fick, M., and Aggelis, G., 2004 .The effect of raw glycerol concentration on the production of 1,3-propanediol by *Clostridium butyricum*. Journal of Chemical Technology and Biotechnology, 79, 1189-1196.

Pijuan, M.,Saunders, A.M., Guisasola, A., Baeza, J.A., Casa, C., and Blackall, L.L., 2004. Enhanced biological phosphorus removal in a sequencing batch reactor using propionate as the sole carbon source. Biotechnology Bioengineering, 85, 56-67.

Popsecu, F., and Lonel, L., 2011. Waste animal fats with high FFA as a renewable energy source for biodiesel production-concept, experimental production and impact evaluation on air quality. Alternative Fuel, Dr. Maximino Manzanera (Ed.), ISBN: 978-953-307-372-9, InTech, DOI: 10.5772/20409.

Randall, A.A., Benefield, L.D., Hill, W.E., Nicol, J.P., Boman, G.K., and Jling, S.R., 1997. The effect of volatile fatty acids on enhanced biological phosphorus removal and population structure in anaerobic/aerobic sequencing batch reactors. Water science Technology, 35, 153-160.

Randall, A.A., and Liu, Y.H., 2002. Polyhydroxyalkanoates form potentially a key aspect of aerobic phosphorus uptake in enhanced biological phosphorous removal. Water Resource, 36, 3473-3478.

Randall, C.W., Barnard, J.L., and Stensel, H.D., 1992. Design and retrofit of wastewater treatment plants for biological nutrient removal. Water Quality Management Library, 5, Technomic Publishing Company, Lancaster, PA,

Randall, E.W., Wilkinson, A., and Ekama, G.A., 1999. An instrument for the direct determination of oxygen utilisation rate. Water SA, 17, 11-18.

Retfalvi, T., Hajos, A.T., Albert, L., and Marosvolgyi, B., 2011. Laboratory scale examination of the effects of overloading on the anaerobic digestion by glycerol. Bioresource Technology, 102, 5270-5275.

Rossle, W.H., and Pretorius, W.A., 2001. A review of characterization requirements for in-line prefermenters Paper 1: Wastewater characterization. Water SA, 27, 405-412.

Saito, T., Brdjanovic, D., and van Loosdrecht, M.C.M., 2004 Effect of nitrite on phosphate uptake by phosphate accumulating organisms. Water Research, 38, 3760-3768.

Sattayasamitsathit, S., Methacanon, P., and Prasertsan, P., 2011. Enhance 1,3-propanediol production from crude glycerol in batch and fed-batch fermentation with two phase pH-controlled strategy. Electronic journal of Biotechnology, 14, 4-4.

Schuchardta, U., Serchelia, R., and Vargas, R.M., 1998. Transesterification of Vegetable oils: a review. Journal of Brazilian Chemical Society, 9, 199-210.

Schuler, A.J., and Jenkins, D., 2003. Enhanced biological phosphorus removal from wastewater by biomass with different phosphorus contents, Part I: Experimental results and comparison with metabolic models. Water Environment Science, 75, 485-498.

Seviour, J., R., Mino, T., and Onuki, M., 2003 The microbiology of biological phosphorus removal in activated sludge systems. FEMS Microbiology Reviews, 27, 99-127.

Sheping, W., Lifang, Y., Guanghui, H., Hairong, Z., and Dangcong, P., 2006. A pilot study on a step-feeding anoxic/oxic activated sludge system. Water Science and Technology, 53, 95-101.

Songliu, L.U., Hongying, H.U., Yingxue, S., and Jia, Y., 2009. Effect of carbon source on the denitrification in constructed wetlands. Journal of Environmental Sciences, 21, 1036-1043.

Sperandio, M., and Paul, E.,2000. Estimation of wastewater biodegradable COD fractions by combining respirotmetric experiments in various S_o/X_o ratios. Water Research, 34, 1233-1246.

Stephens, H., 2004. Comprehensive analysis of full-scale enhance biological phosphorus removal facilities. WEFTEC 77th Annual Technical Exhibition and Conference, October 2–6, 2004, New Orleans, Session 83.

Tasli, R., Orhon, D., and Artan, N., 1999. The effect of substrate composition on the nutrient removal potential of sequencing batch reactors. Waster SA, 25, 337-344.

Taya, C., Guerrero, J., Suarez-Ojeda, M, E., Guisasola, A., and Baeza, J, A., 2015 Assessment of crude glycerol for Enhanced Biological Phosphorus Removal: Stability and role of long chain fatty acids. Chemosphere, 141, 50-56.

Taya, C., Guerrero, J., Vanneste, G., Guisasola, A., and Baeza, J.A., 2012. Methanol-Driven Enhanced Biological Phosphours Removal with a syntrophic consortium. Biotechnology and Bioengineering, 110, 391-400.

Uprety, K., Charles, B., Chris, B., Kevin, P., Bill, B., Katya, B., and Ron, L., 2012. Glycerol-driven denitrification: Evaluating the specialist-generalist theory and partial denitrification to nitrite. Water Environment Federation Session, 51-60, 3747-3771.

Uprety, K., 2013. Evaluation of Glycerol and Waste Alcohol as Supplemental Carbon Sources for Denitrification Partial fulfillment for the requirement of Master Thesis. Virginia Polytechnic Institute and State University

Viana. M.B., Freitas, A.V., Leitao, R.C., Pinto, G.A.S., and Santaella, S.T. 2012 Anaerobic digestion of crude glycerol: a review. Environmental Technology Review, 1, 81-92.

Vollertsen, J., and Jacobsen, T.H., 2002. Biodegradability of wastewater- a method for COD-fractionation. Water Science Technology, 45, 25-34.

Wentzel M.C., Dold P.L., Ekama G.A., and Marais G.v.R., 1990. Biological excess phosphorus removal - Steady state process design. Water SA, 16, 29-48.

Wentzel, M.C., Ekama, G.A., and Marais, G.v.R., 1992. Process and modelling of nitrification denitrification biological excess phosphorus biological excess phosphorus removal systems-a review. Water Science Technology, 25, 59-82.

Wentzel, M.C., Mbewe, A., and Ekama, G. A., 1995. Batch test for measurement of readily biodegradable COD and active organism concentrations in municipal wastewaters. Water SA, 21, 117-123.

Werkman, C.H., and Gillen, G.F., 1932. Bacteria producing trimethylene glycol. Journal Bacteriology, 23, 167-182.

Yazdani, S.S., and Gonzalez, R., 2007. Anaerobic fermentation of glycerol: a path to economic vialbility for the biofuels industry. Current option in biotechnology, 18, 213-219.

Yuan., Q., 2011. Fermentation –Enhanced Sustainable Biological Phosphorus Removal. In partial fulfillment of the requirements of the degree of DOCTOR OF PHILOSOPHY, University of Manitoba.

Yuan, Q., Sparling, P. L., Lee, M., Taniguchi, D., and Oleszkiewicz, J.A., 2010. Enhancing biological phosphorus removal with glycerol. Water Science and Technology, 61, 1837-1843.

Ziglio, G., Andreottola, G., Foladori, P., and Ragazzi, M., 2001. Experimental Validation of a single-Our method for wastewater RBCOD characterization. Water science and Technology, 43, 119-126.